Electronic Supplementary Material (ESI) for Catalysis Science & Technology.

Supporting Information

Investigations into the influence of nickel loading on MoO_3-modified catalysts for the gas-phase hydrodeoxygenation of anisole

Simon Haida, Sebastian Löbner, Henrik Lund, Stephan Bartling, Carsten Kreyenschulte, Hanan Atia, Ali M. Abdel-Mageed, Christoph Kubis* and Angelika Brückner*

*E-mail: christoph.kubis@catalysis.de, angelika.brueckner@catalysis.de

Supporting Information - Table of Contents

SI-A: Additional experimental part

Pseudo in situ X-ray photoelectron spectroscopy (XPS) measurements were performed in a laboratory Near Ambient Pressure (NAP) X-ray photoelectron spectroscopy system (NAP-XPS, SPECS Surface Nano Analysis GmbH, Germany). The setup is equipped with a differentially pumped Phoibos 150 electron energy analyser and a monochromated Al Kα radiation source (E = 1486.6 eV) operated at 70 W and 15 kV. The system is connected to a High-Pressure Cell (HPC 20, SPECS Surface Nano Analysis GmbH, Germany) which offers sample heating by a halogen lamp (up to 800 °C) and is equipped with 4 mass flow controllers (MFC's) at the gas inlet and a manual back pressure regulator (Swagelok, USA) at the outlet. For the current experiments at ambient pressure conditions the samples were heated with 10 K/min to 325°C in N_2. Then the desired gas mixture (H_2, CH_4:H_2) was applied for different times before the sample was cooled down in N_2 again. The cell was evacuated, and the sample could be transferred under vacuum to the measurement chamber. The powder samples are pressed on a stainless-steel sample plate using a laboratory press with 5 mm diameter and a load of about 0.5 t. Temperature is monitored by a thermocouple on the sample plate pressed to the sample surface. The electron binding energies are referenced to the C 1s core level of carbon at 284.8 eV (C-C and C-H bonds). For analysis, the peaks were deconvolved with Gaussian-Lorentzian curves using the software Unifit 2023.

Si-B: Catalytic results

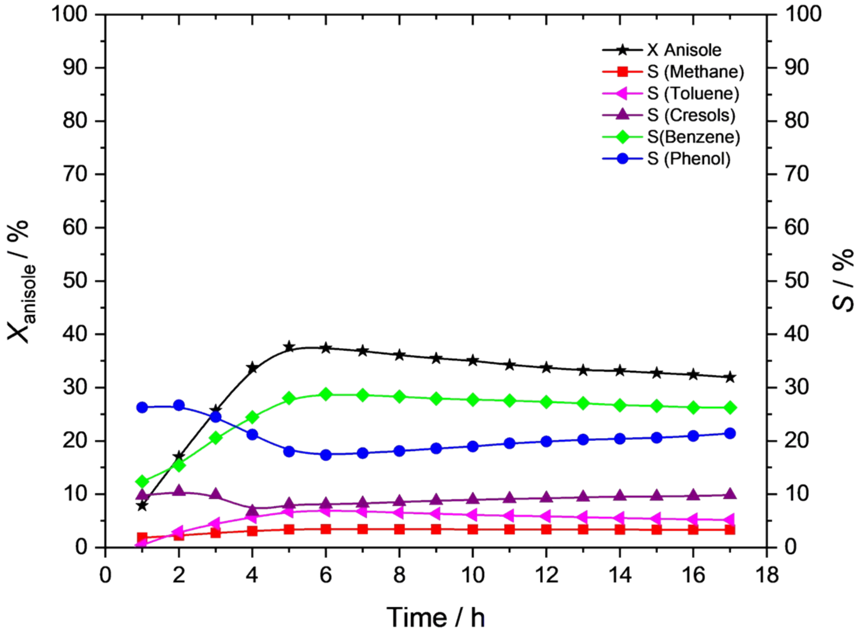

Figure SI 1: Averaged conversion and selectivities of the relevant compounds for MoO_3 at T = 325 °C, pre-reduced in 100 % H_2 for 2 h at 325 °C, WHSV = 0.31 $g_{anisole} \cdot g^{-1}{}_{cat} \cdot h^{-1}$, particle size = 600-800 µm, 200 mg cat. diluted with 2.3 g quartz.

Table SI 1: Single run catalytic performance data. Catalyst: MoO_3. Anisole conversion and product selectivities (C-mol%) at 325 °C, WHSV = 0.31 $g_{anisole} \cdot g^{-1}{}_{cat} \cdot h^{-1}$ and TOS = 10 h.

Nr.	X(Anisole)	S(Methane)	S(Benzene)	S(Toluene)	S(Xylenes)	S(Phenol)	S(Cresols)	S(Uncalibrated)	C Yield
1	39.76	3.71	30.23	6.57	2.06	19.41	8.93	7.98	96.4
2	34.74	3.64	30.08	7.14	2.28	17.02	7.69	7.31	94.6
3	34.41	3.23	26.35	6.01	1.81	18.13	8.41	7.63	95.1
4	36.14	3.10	25.32	5.63	1.74	17.77	9.09	8.25	94.3
5	32.20	3.40	27.63	6.33	2.08	20.54	9.74	8.24	97.4

S(Uncalibrated): Unknown compounds, response factor for anisole used for calculation.

C Yield: Ratio of sum of all integral values of all components including not-converted anisole during catalytic reaction divided by the integral value of initial anisole feed.

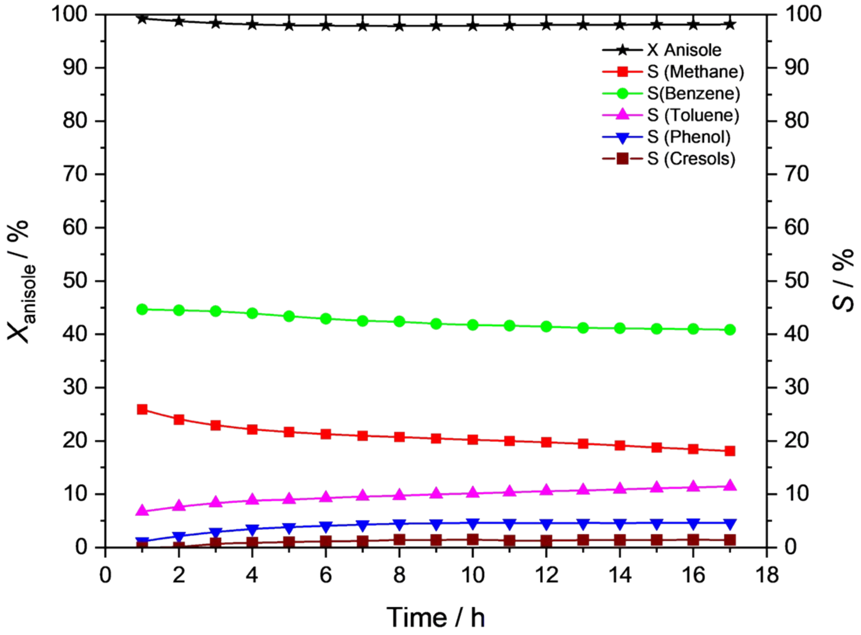

Figure SI 2: Averaged conversion and selectivities of the relevant compounds for $NiMoO_4$ at T = 325 °C, pre-reduced in 100 % H_2 for 2 h at 325 °C, WHSV = 0.31 $g_{anisole}\cdot g^{-1}{}_{cat}\cdot h^{-1}$, particle size = 600-800 µm, 200 mg cat. diluted with 2.3 g quartz.

Table SI 2: Single run catalytic performance data. Catalyst: $NiMoO_4$. Anisole conversion and product selectivities (C-mol%) at 325 °C, WHSV = 0.31 $g_{anisole}\cdot g^{-1}{}_{cat}\cdot h^{-1}$ and TOS = 10 h.

Nr.	**X(Anisole)**	**S(Methane)**	**S(Benzene)**	**S(Toluene)**	**S(Xylenes)**	**S(Phenol)**	**S(Cresols)**	**S(Uncalibrated)**	**C Yield**
1	97.71	20.88	41.52	9.92	2.88	4.29	1.38	2.57	98.2
2	98.11	19.98	42.42	10.05	2.83	4.69	1.41	2.36	98.5

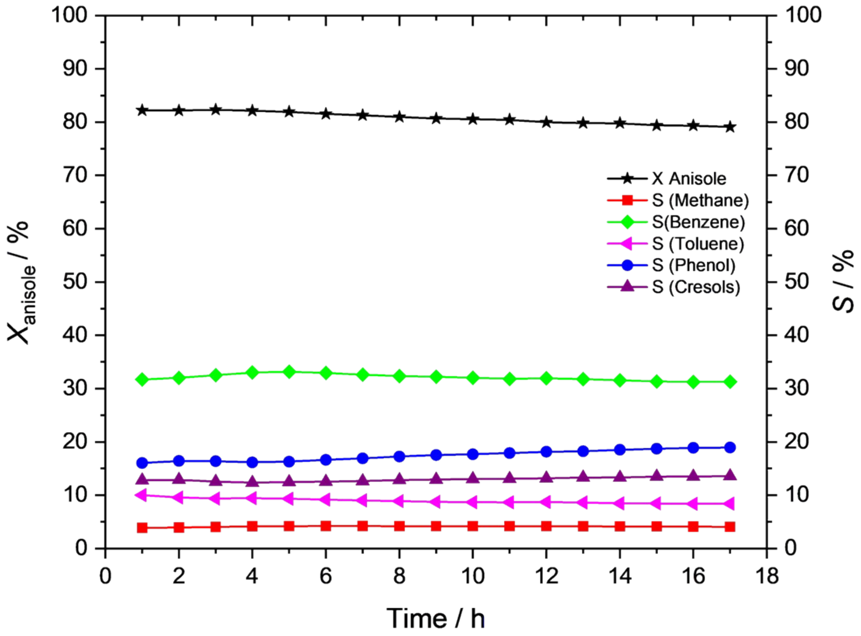

Figure SI 3: Averaged conversion and selectivities of the relevant compounds for Ni(5)MoO_3 at T = 325 °C, pre-reduced in 100 % H_2 for 2 h at 325 °C, WHSV = 0.31 $g_{anisole}$ $g^{-1}_{cat}\cdot h^{-1}$, particle size = 600-800 µm, 200 mg cat. diluted with 2.3 g quartz.

Table SI 3: Single run catalytic performance data. Catalyst: Ni(5)MoO_3. Anisole conversion and product selectivities (C-mol%) at 325 °C, WHSV = 0.31 $g_{anisole}\cdot g^{-1}_{cat}\cdot h^{-1}$ and TOS = 10 h.

Nr.	**X(Anisole)**	**S(Methane)**	**S(Benzene)**	**S(Toluene)**	**S(Xylenes)**	**S(Phenol)**	**S(Cresols)**	**S(Uncalibrated)**	**C Yield**
1	80.98	4.16	32.24	8.87	3.12	16.91	12.83	9.11	101.8
2	81.25	4.24	32.58	8.87	3.18	17.57	12.74	9.36	101.7

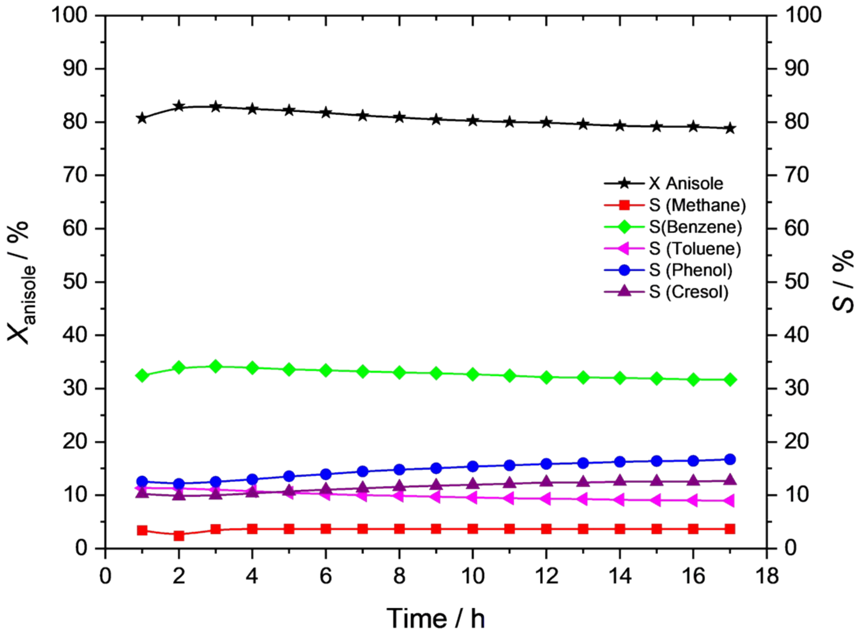

Figure SI 4: Averaged conversion and selectivities of the relevant compounds for Ni(3)MoO_3 at T = 325 °C, pre-reduced in 100 % H_2 for 2 h at 325 °C, WHSV = 0.31 $g_{anisole}\cdot g^{-1}_{cat}\cdot h^{-1}$, particle size = 600-800 µm, 200 mg cat. diluted with 2.3 g quartz.

Table SI 4: Single run catalytic performance data. Catalyst: Ni(3)MoO_3. Anisole conversion and product selectivities (C-mol%) at 325 °C, WHSV = 0.31 $g_{anisole}\cdot g^{-1}_{cat}\cdot h^{-1}$ and TOS = 10 h.

Nr.	X(Anisole)	S(Methane)	S(Benzene)	S(Toluene)	S(Xylenes)	S(Phenol)	S(Cresols)	S(Uncalibrated)	C Yield
1	79.23	3.69	33.68	10.29	3.9	13.94	11.05	7.96	100.7
2	81.28	3.67	32.76	9.70	3.45	15.57	12.08	8.95	101.7
3	80.91	3.69	32.22	9.11	3.22	15.63	12.16	8.65	99.6

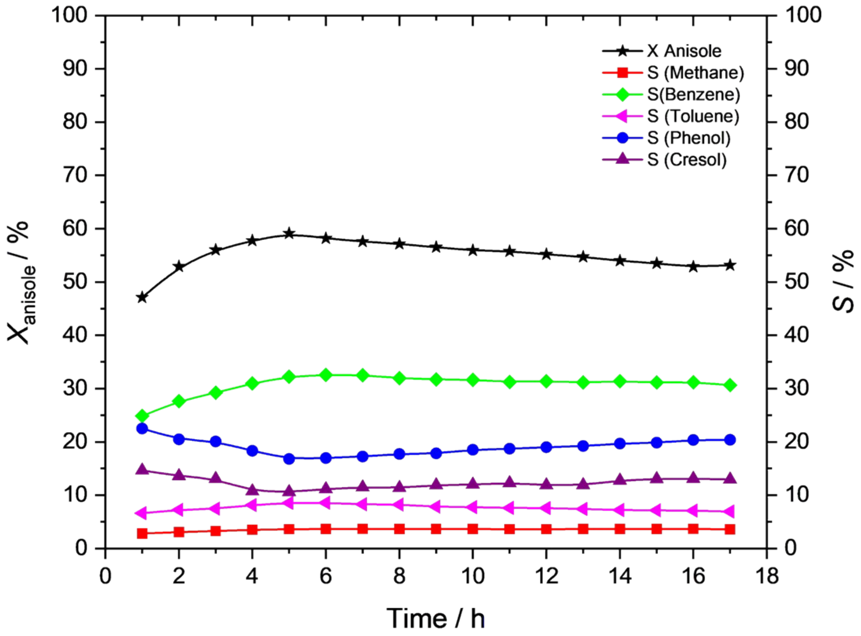

Figure SI 5: Averaged conversion and selectivities of the relevant compounds for Ni(1)MoO_3 at T = 325 °C, pre-reduced in 100 % H_2 for 2 h at 325 °C, WHSV = 0.31 $g_{anisole}\cdot g^{-1}_{cat}\cdot h^{-1}$, particle size = 600-800 µm, 200 mg cat. diluted with 2.3 g quartz.

Table SI 5: Single run catalytic performance data. Catalyst: Ni(1)MoO_3. Anisole conversion and product selectivities (C-mol%) at 325 °C, WHSV = 0.31 $g_{anisole}\cdot g^{-1}_{cat}\cdot h^{-1}$ and TOS = 10 h.

Nr.	X(Anisole)	S(Methane)	S(Benzene)	S(Toluene)	S(Xylenes)	S(Phenol)	S(Cresols)	S(Uncalibrated)	C Yield
1	56.15	3.39	30.22	7.51	2.51	19.28	12.31	9.04	99.1
2	56.86	3.89	33.24	8.15	3.21	16.39	11.46	9.69	99.6

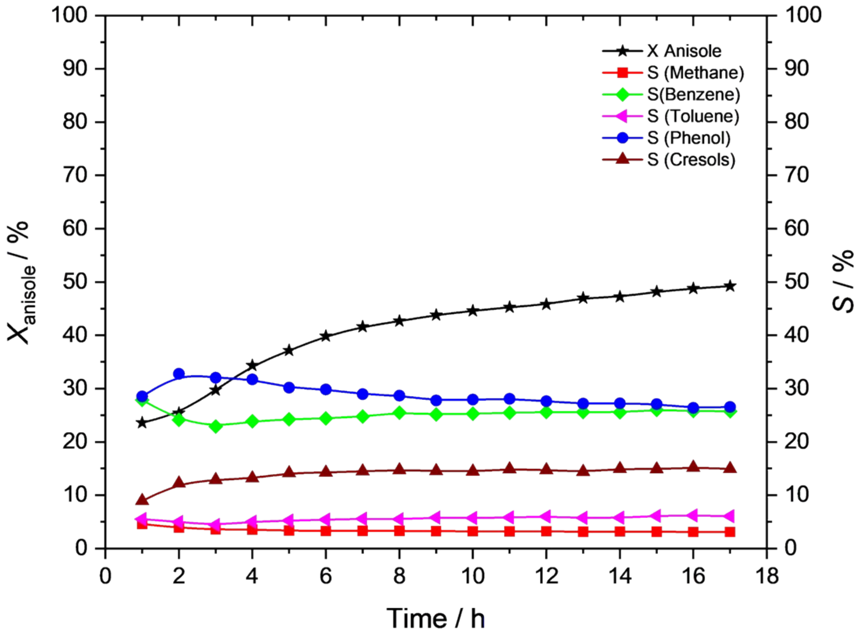

Figure SI 6: Conversion and selectivities of the relevant compounds for $CoMoO_4$ at T = 325 °C, pre-reduced in 100 % H_2 for 2 h at 325 °C, WHSV = 0.31 $g_{anisole} \cdot g^{-1}_{cat} \cdot h^{-1}$, particle size = 600-800 µm, 200 mg cat. diluted with 2.3 g quartz.

Table SI 6: $CoMoO_4$ Anisole conversion and product selectivities (C-mol%) at 325 °C, WHSV = 0.31 $g_{anisole} \cdot g^{-1}_{cat} \cdot h^{-1}$ and TOS = 10 h.

Nr.	**X(Anisole)**	**S(Methane)**	**S(Benzene)**	**S(Toluene)**	**S(Xylenes)**	**S(Phenol)**	**S(Cresols)**	**S(Uncalibrated)**	**C Yield**
1	44.6	3.23	25.29	5.70	2.04	27.93	14.46	20.97	104.9

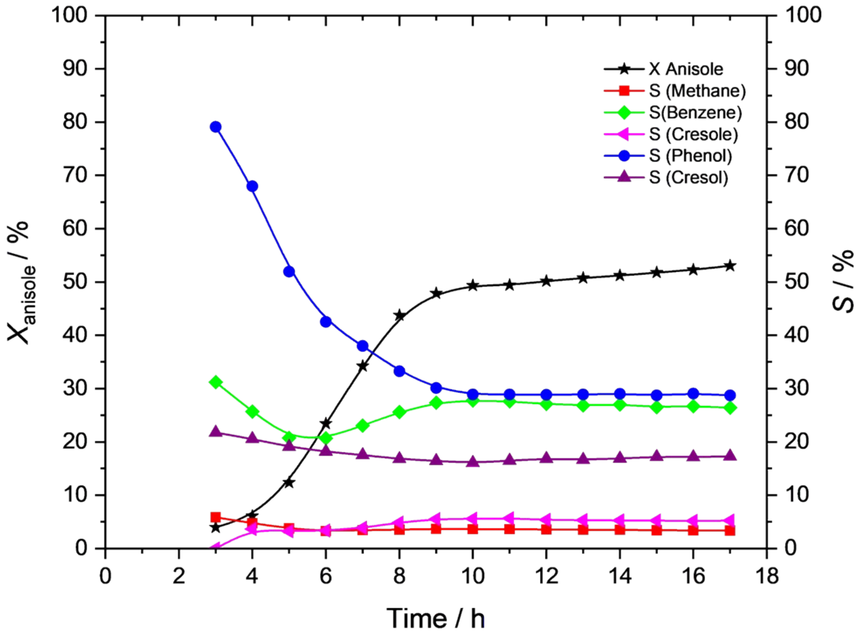

Figure SI 7: Conversion and selectivities of the relevant compounds for Co(5)MoO_3 at T = 325 °C, pre-reduced in 100 % H_2 for 2 h at 325 °C, WHSV = 0.31 $g_{anisole}\cdot g^{-1}_{cat}\cdot h^{-1}$, particle size = 600-800 µm, 200 mg cat. diluted with 2.3 g quartz.

Table SI 7: Co(5)MoO_3 Anisole conversion and product selectivities (C-mol%) at 325 °C, WHSV = 0.31 $g_{anisole}\cdot g^{-1}_{cat}\cdot h^{-1}$ and TOS = 10 h.

Nr.	X(Anisole)	S(Methane)	S(Benzene)	S(Toluene)	S(Xylenes)	S(Phenol)	S(Cresols)	S(Uncalibrated)	C Yield
1	49.33	3.62	27.77	5.57	1.96	28.89	16.07	16.85	105.0

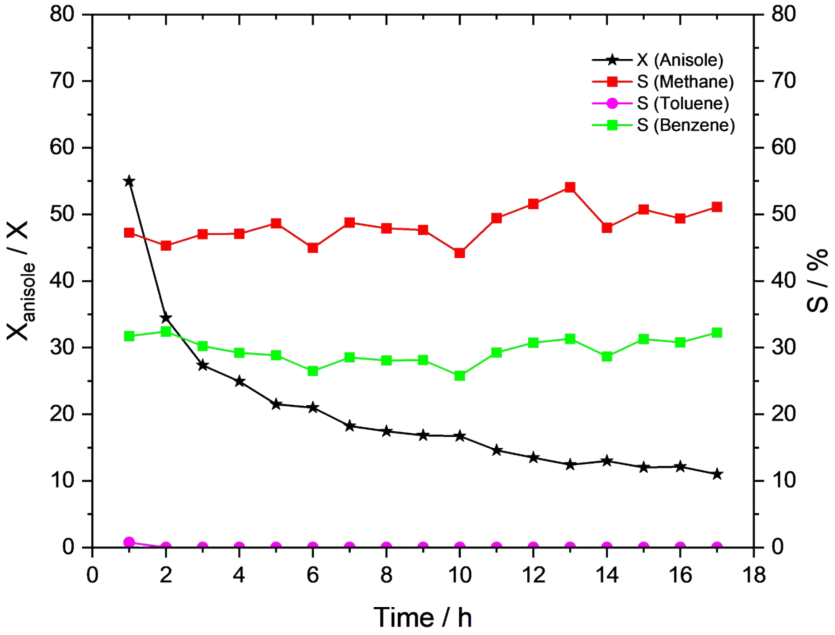

Figure SI 8: Conversion of anisole and selectivities of the relevant products for Ni/α-Al_2O_3 (Ni content: 3 wt.%) as catalyst at T = 325 °C, pre-reduced in 100 % H_2 for 2 h at 325 °C, WHSV = 0.31 $g_{anisole}\cdot g^{-1}{}_{cat}\cdot h^{-1}$, particle size = 600-800 µm, 200 mg cat. diluted with 2.3 g quartz.

Table SI 8: Single run catalytic performance data. Catalyst: Ni/α-Al_2O_3 (Ni content: 3 wt.%). Anisole conversion and product selectivities (C-mol%) at 325 °C, WHSV = 0.31 $g_{anisole}\cdot g^{-1}{}_{cat}\cdot h^{-1}$ and TOS = 10 h.

Nr.	X(Anisole)	S(Methane)	S(Benzene)	S(Toluene)	S(Xylenes)	S(Phenol)	S(Cresols)	S(Uncalibrated)	C Yield
1	16.71	44.19	25.76	0.00	0.00	0.00	0.00	0.00	96.1

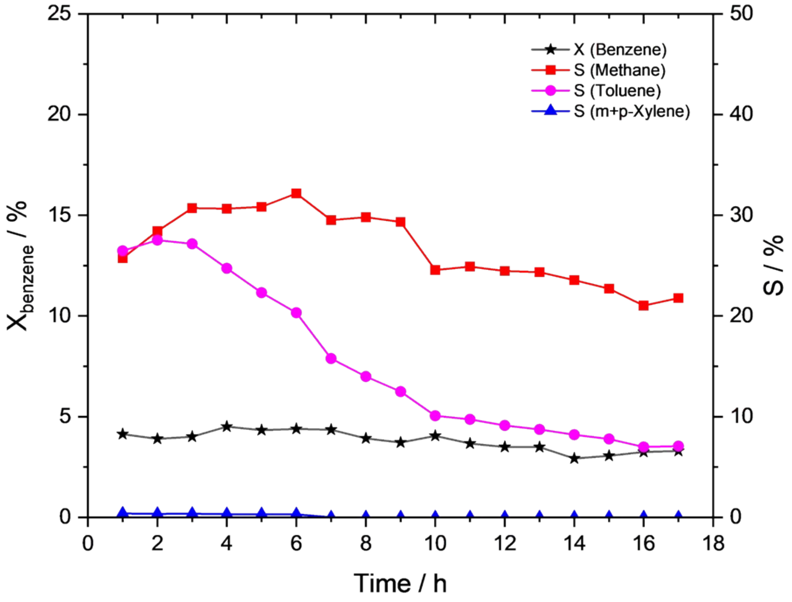

Figure SI 9: Conversion of benzene and product selectivities for $NiMoO_4$ as catalyst at T = 325 °C, pre-reduced in 100 % H_2 for 2 h at 325 °C, WHSV = 6.30 $g_{benzene}\cdot g^{-1}_{cat}\cdot h^{-1}$, particle size = 600-800 µm, 200 mg cat. diluted with 2.3 g quartz.

Table SI 9: Single run catalytic performance data. Catalyst: $NiMoO_4$. Benzene conversion and product selectivities (C-mol%) at 325 °C, WHSV = 6.30 $g_{benzene}\cdot g^{-1}_{cat}\cdot h^{-1}$ and TOS = 10 h.

Nr.	**X(Benzene)**	**S(Methane)**	**S(Anisole)**	**S(Toluene)**	**S(Xylenes)**	**S(Phenol)**	**S(Cresols)**	**S(Uncalibrated)**	**C Yield**
1	4.05	21.05	0.00	8.64	0.00	0.00	0.00	2.53	97.4

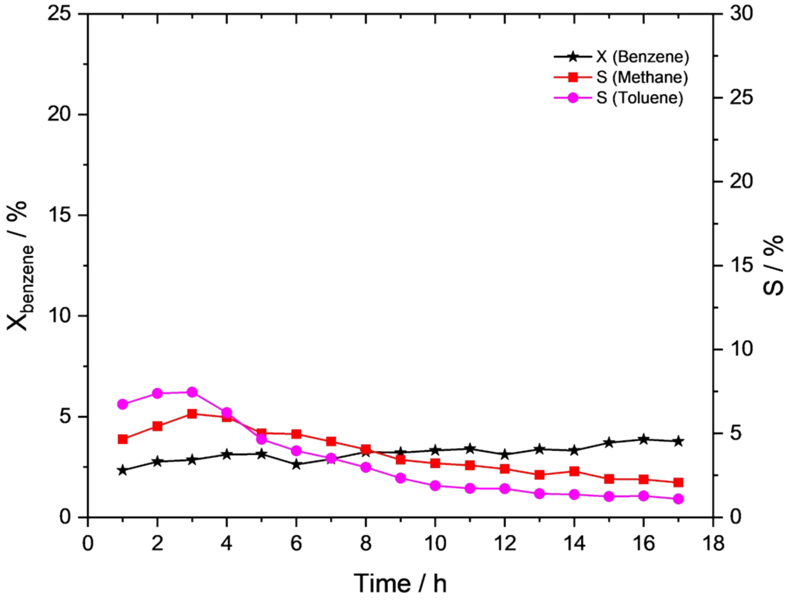

Figure SI 10: Conversion of benzene and product selectivities for Ni(5)MoO_3 as catalyst at T = 325 °C, pre-reduced in 100 % H_2 for 2 h at 325 °C, WHSV = 6.30 $g_{benzene}\cdot g^{-1}{}_{cat}\cdot h^{-1}$, particle size = 600-800 µm, 200 mg cat. diluted with 2.3 g quartz.

Table SI 10: Single run catalytic performance data. Catalyst: Ni(5)MoO_3. Benzene conversion and product selectivities (C-mol%) at 325 °C, WHSV = 6.30 $g_{benzene}\cdot g^{-1}{}_{cat}\cdot h^{-1}$ and TOS = 10 h.

Nr.	X(Benzene)	S(Methane)	S(Anisole)	S(Toluene)	S(Xylenes)	S(Phenol)	S(Cresols)	S(Uncalibrated)	C Yield
1	3.32	2.76	0.00	1.62	0.00	0.00	0.00	0.97	97.8

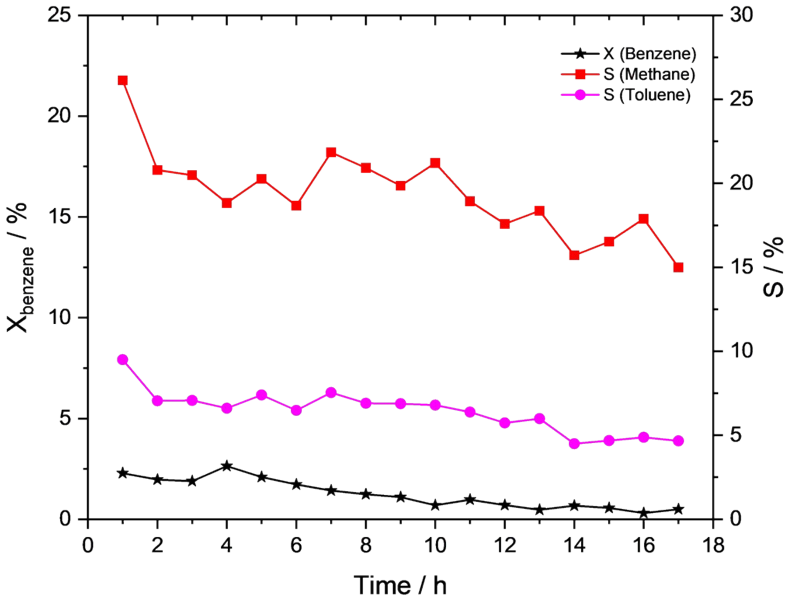

Figure SI 11: Conversion of benzene and product selectivities for Ni/α-Al_2O_3 (Ni content: 3 wt.%) as catalyst at T = 325 °C, pre-reduced in 100 % H_2 for 2 h at 325 °C, WHSV = 6.30 $g_{benzene}\cdot g^{-1}{}_{cat}\cdot h^{-1}$, particle size = 600-800 µm, 200 mg cat. diluted with 2.3 g quartz.

Table SI 11: Single run catalytic performance data. Catalyst: Ni/Al_2O_3 (Ni content: 3 wt.%). Benzene conversion and product selectivities (C-mol%) at 325 °C, WHSV = 6.30 $g_{benzene}\cdot g^{-1}{}_{cat}\cdot h^{-1}$ and TOS = 10 h.

Nr.	X(Benzene)	S(Methane)	S(Anisole)	S(Toluene)	S(Xylenes)	S(Phenol)	S(Cresols)	S(Uncalibrated)	C Yield
1	0.69	18.17	0.00	5.82	0.00	0.00	0.00	0.78	98.9

SI-C: BET-surface areas

Table SI 12: BET-surface areas of fresh and spent samples

Sample	**Fresh catalyst [m²/g]**	**Spent catalyst [m²/g]**
MoO_3	3	7
Ni(5)MoO_3	15	18
$NiMoO_4$	40	32

SI-D: Scanning electron microscopy

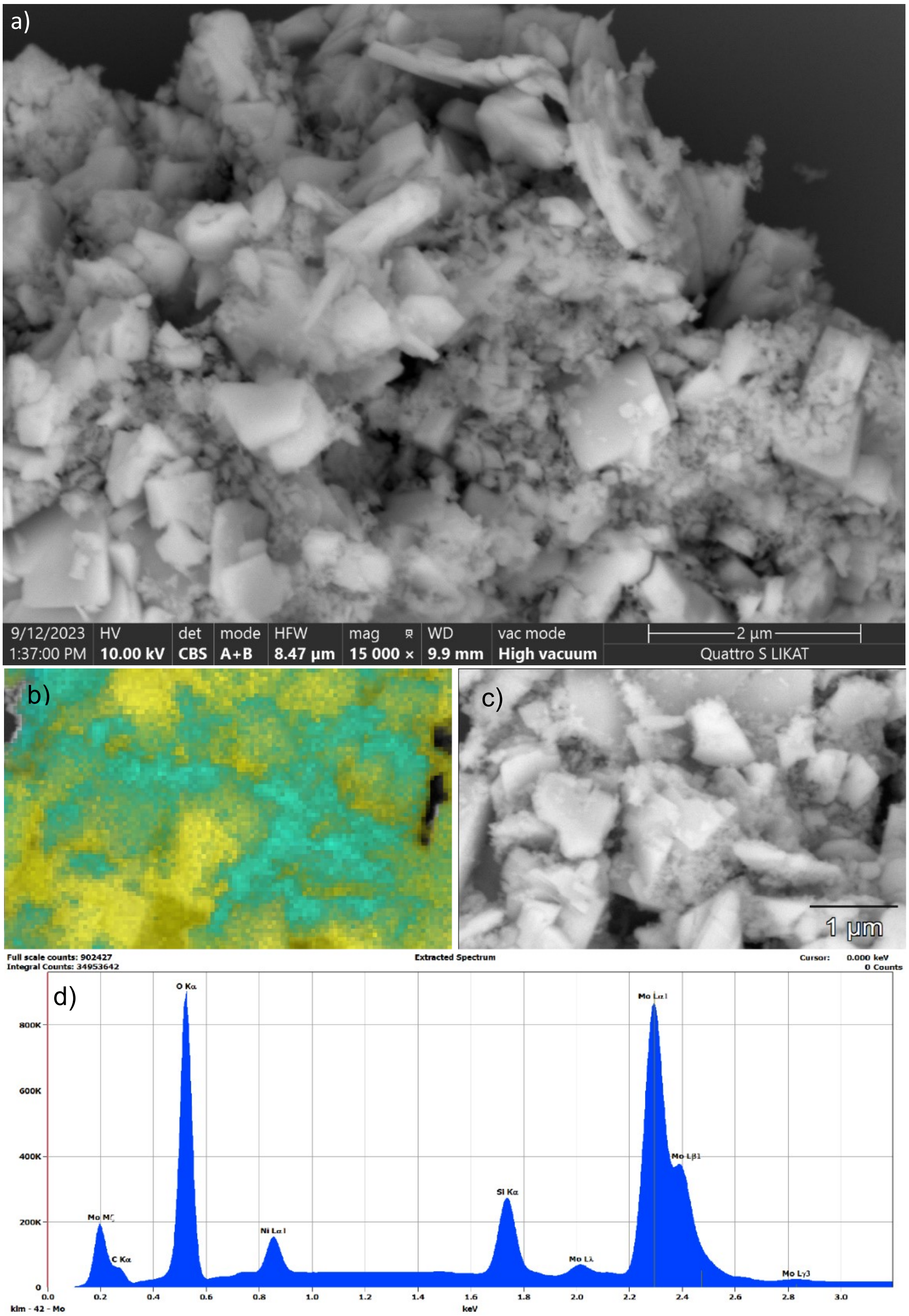

Figure SI 12: SEM overview images in BSE mode of fresh Ni(5)MoO_3 a) SEM image b) overlaid with the color image of the elemental distributions of Mo (yellow) and Ni (cyan) calculated from the EDX spectra from the area of c) and d) the EDX spectra of fresh Ni(5)MoO_3.

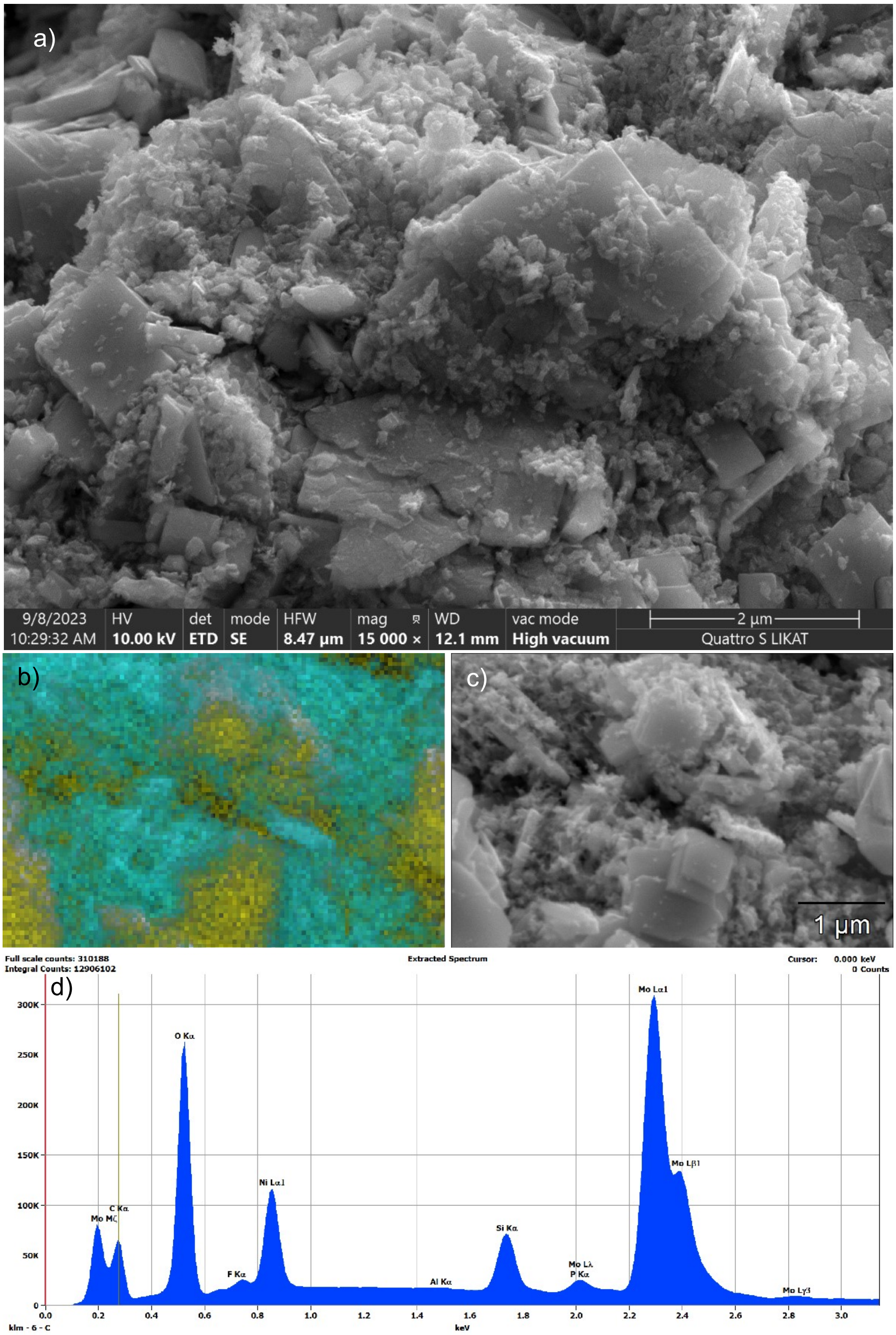

Figure SI 13: SEM overview images in SE mode of spent Ni(5)MoO_3 a) SEM image b) overlaid with the color image of the elemental distributions of Mo (yellow) and Ni (cyan) calculated from the EDX spectra from the area of c) and d) the EDX spectra of spent Ni(5)MoO_3.

SI-E: TG-MS

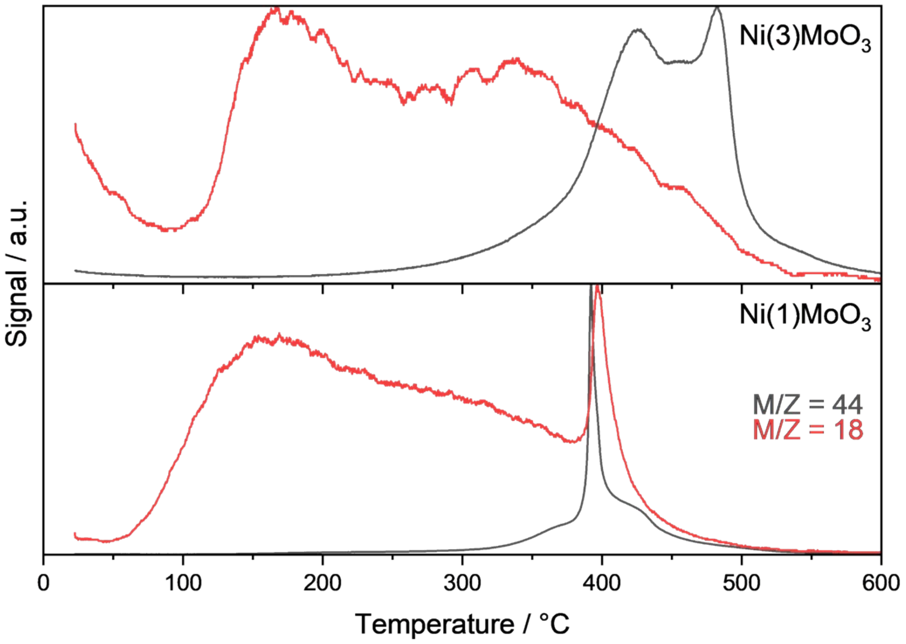

Figure SI 14: TG-MS measurement of spent catalysts in syn. air with a temperature ramp of 10 °C/min.

SI-F: Ni2p XP spectra of spent catalysts

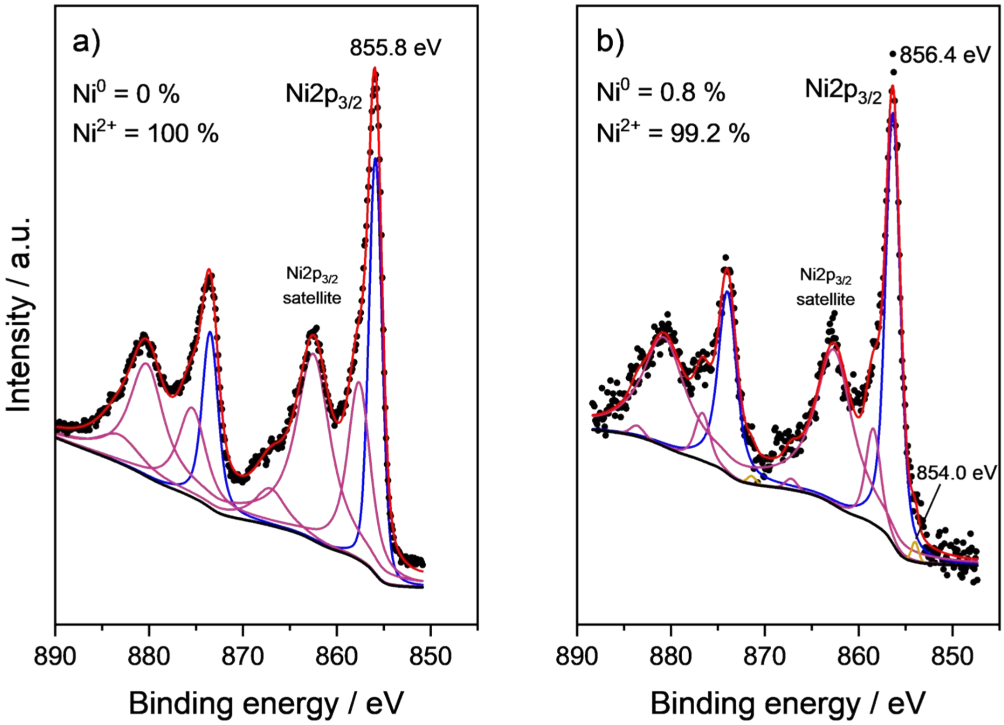

Figure SI 15: Ni 2p XP spectra of a) fresh Ni(5)MoO_3 b) spent Ni(5)MoO_3 after 17 h TOS at 325 °C.

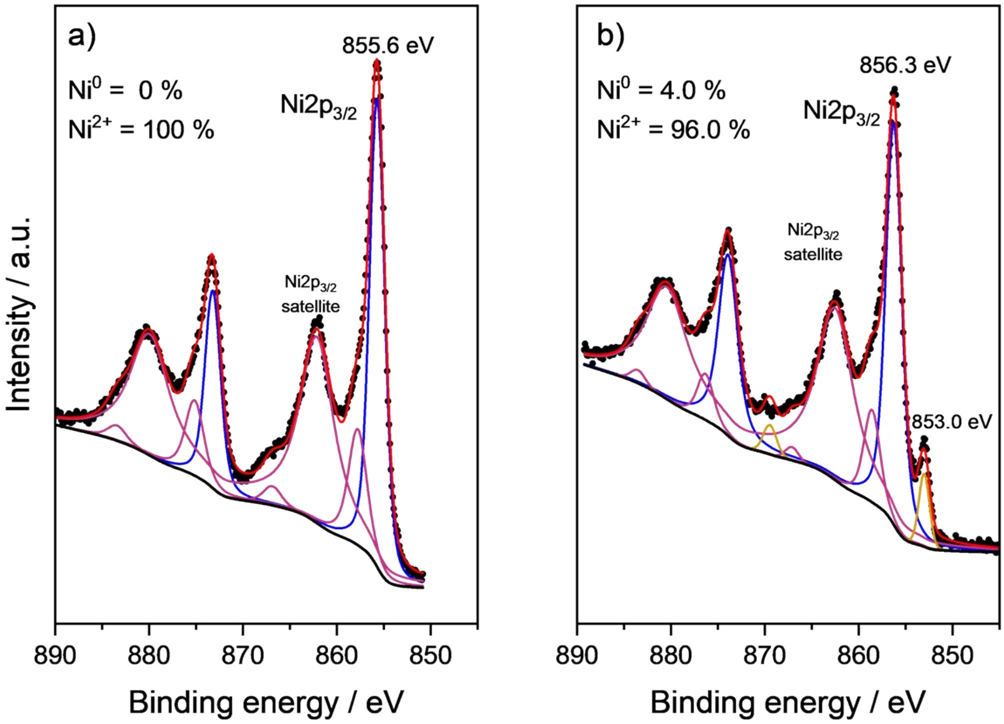

Figure SI 16: Ni 2p XP spectra of a) fresh $NiMoO_4$ b) spent $NiMoO_4$ after 17 h TOS at 325 °C.

SI-G: Pseudo in-situ XPS experiments

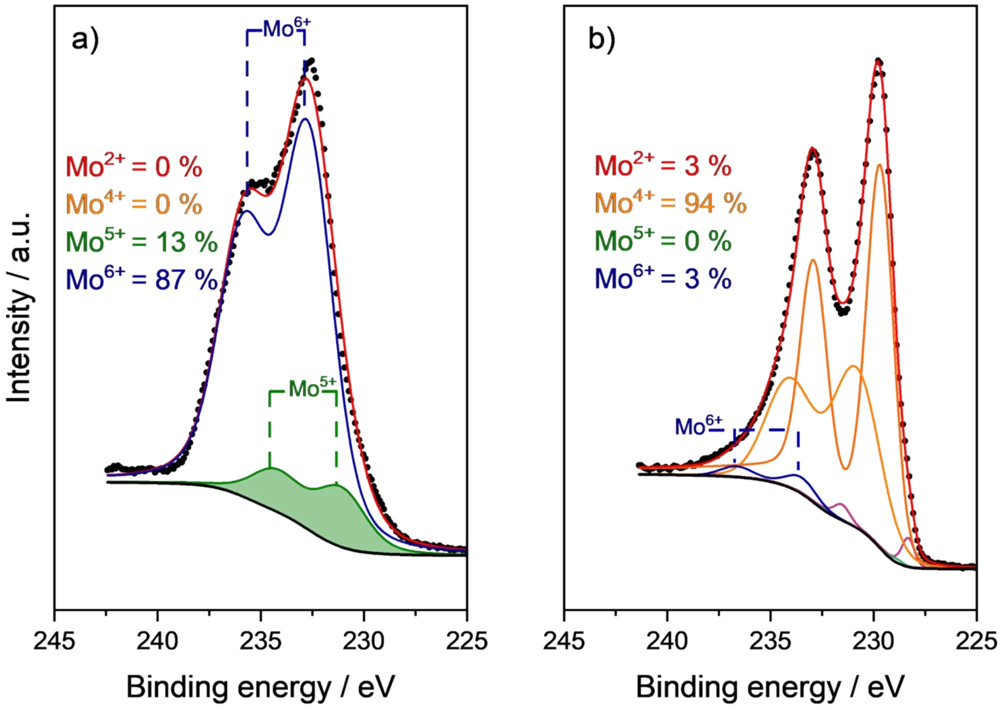

Figure SI 17: Mo3d Pseudo in-situ XP spectra. a) fresh $NiMoO_4$ b) $NiMoO_4$ after reduction in 100 % H_2 for 2 h at 325 °C.

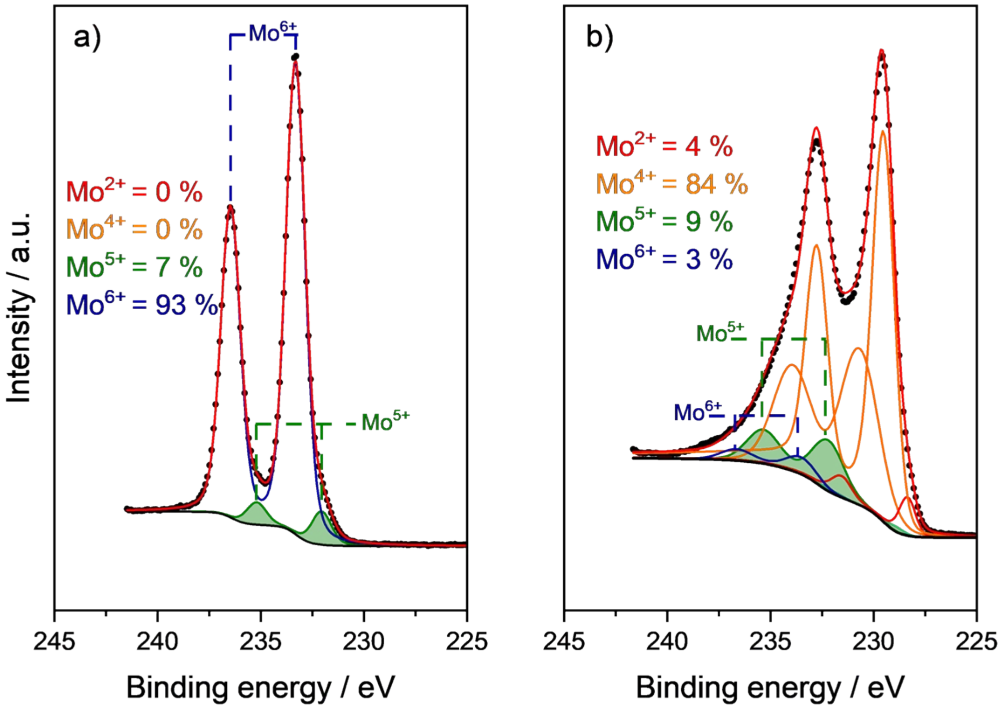

Figure SI 18: Mo3d Pseudo in-situ XP spectra. a) fresh Ni(5)MoO_3 b) Ni(5)MoO_3 after reduction in 100 % H_2 for 2 h at 325 °C.

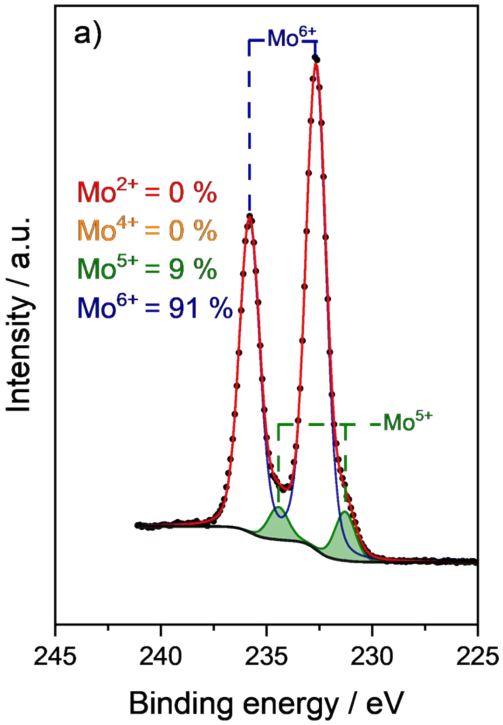

Figure SI 19: Mo3d Pseudo in-situ XP spectra. a) fresh MoO_3 b) MoO_3 after reduction in 100 % H_2 for 2 h at 325 °C.

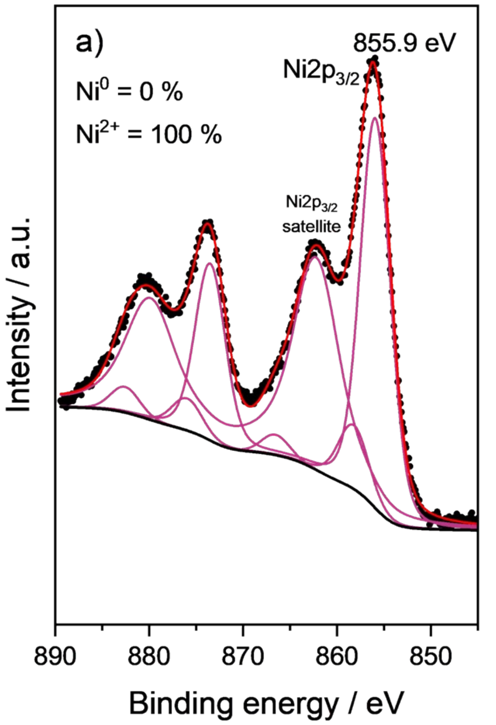

Figure SI 20: Ni 2p pseudo in-situ XP spectra. a) fresh $NiMoO_4$ b) $NiMoO_4$ after reduction in 100 % H_2 for 2 h at 325 °C.

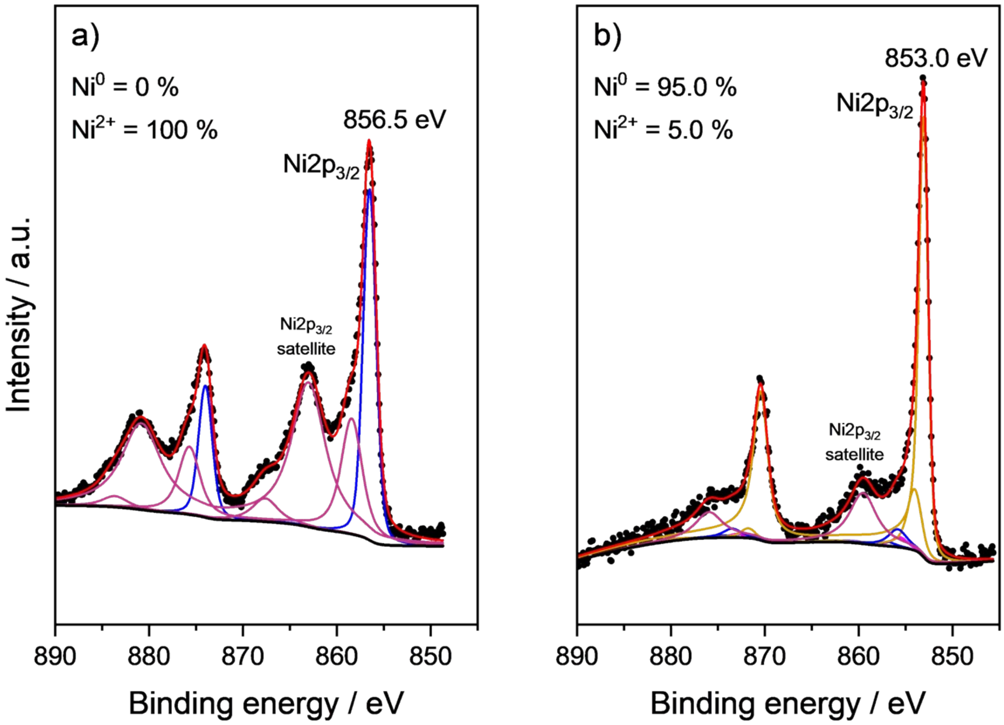

Figure SI 21: Ni 2p pseudo in-situ XP spectra. a) fresh Ni(5)MoO_3 b) Ni(5)MoO_3 after reduction in 100 % H_2 for 2 h at 325 °C.

SI-H: TPR of fresh catalysts

Temperature programmed reduction (TPR) measurements were performed in a 3-Flex with a quartz tube reactor and a thermal conductivity detector for quantification. Around 50 mg of the samples were loaded in the reactor and pretreated at 400 °C (20 K/min) under the flow of 5%O_2/He for 30 min to remove any adsorbed species on the surface of the samples. After then, the sample is cooled to RT under Ar flow. Then, the flow was changed to 50 ml/min H_2/Ar and the sample was then ramped to 850 °C at a heating rate of 10 K/min. The temperature was held at 850 °C for 90 min. The hydrogen consumption peaks were recorded with temperature and quantitative analysis of the TPR data, based on the peak areas, was calculated after calibration.

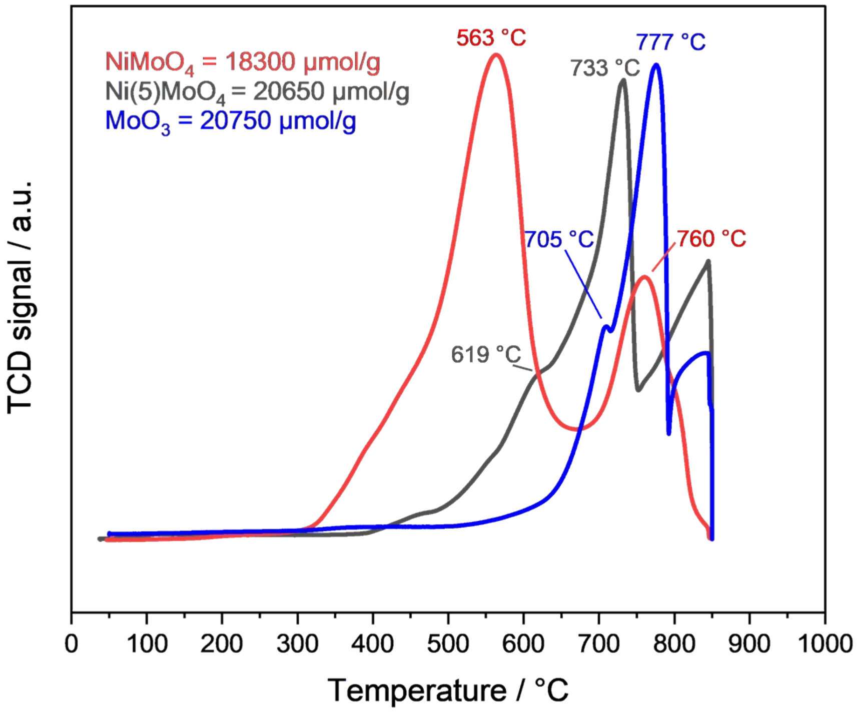

Figure SI 22: TPR of fresh catalysts in 5% H_2 with 10 °C/min; m ≈ 20 mg.

TPR patterns of MoO_3, Ni(5)MoO_4 and $NiMoO_4$ catalysts are presented in Figure SI 16. The reduction peaks appeared in three regions: one started above 300 °C, the next higher than 600 °C and the last at high temperatures above 800 °C. For the MoO_3 sample, the H_2 the reduction starts above 600 °C, and the major consumption peak appeared at 777 °C corresponding to the reduction of MoO_3 to MoO_x (Mo^{5+} and Mo^{4+} species).[1,2] At higher temperature above 800 °C, the peak was assigned to the reduction of MoO_x to metallic Mo^0. For $NiMoO_4$, two characteristic lower reduction peaks compared to MoO_3 and Ni(5)MoO_4 at around 563 and 785 ◦C were observed. The shoulder present in MoO_3 at 705°C is shifted to lower temperature (<400 °C) and its intensity decreased with the increase of Ni content. In this context, incorporation of Ni species, especially with the high content (26 %) as in the sample $NiMoO_4$ all reduction peaks of Mo species shifted to the lower temperature compared with those of MoO_3 alone and/or Ni(5)MoO4 which showed slight shift to lower reduction temperatures. Ni could promote the low-temperature reduction of Mo^{6+} species due to H_2 spill over on the metal active sites.[1,3] The amount of H_2 consumed theoretically for MoO_3 should be 20800, and experimentally 20750 µmol/g was determined indicating full reduction of the MoO_3. The same was found for the Ni doped MoO_3 samples.

1) S. Qiu, Z. Huang, X. Sang, Y. Liu, Q. Zhang, Q. Chen, Q. Meng, T. Wang, *Fuel Process. Technol.* **2023**, *242*, 107647.
2) S. Li, Y. Lv, G. Song, C. Li, D. Gao, G. Chen, *RSC Advances* 2019, **9**, 4571-4582.
3) S. Qiu, T. Wang, Y. Fang, *Fuel Process. Technol.* **2019**, *183*, 19-26.

SI-I: Anisole DRIFTS adsorption experiments

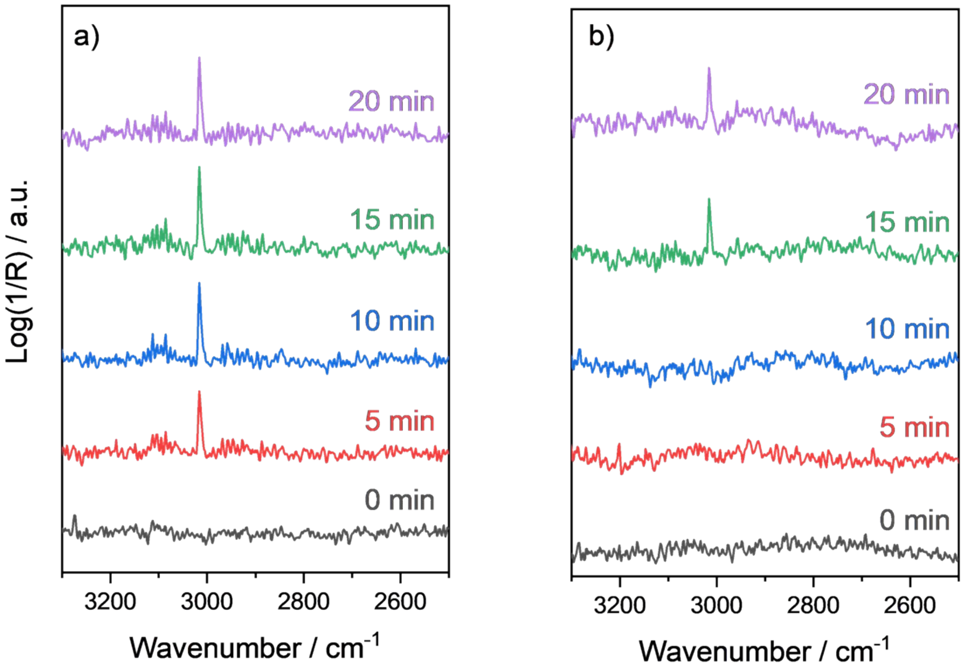

Figure SI 23: Comparison methane evolution after benzene adsorption in He and switch to H_2 at 325 °C and pre-reduction at 325 °C in 100 % H_2 for a) $NiMoO_4$ and $CoMoO_4$.

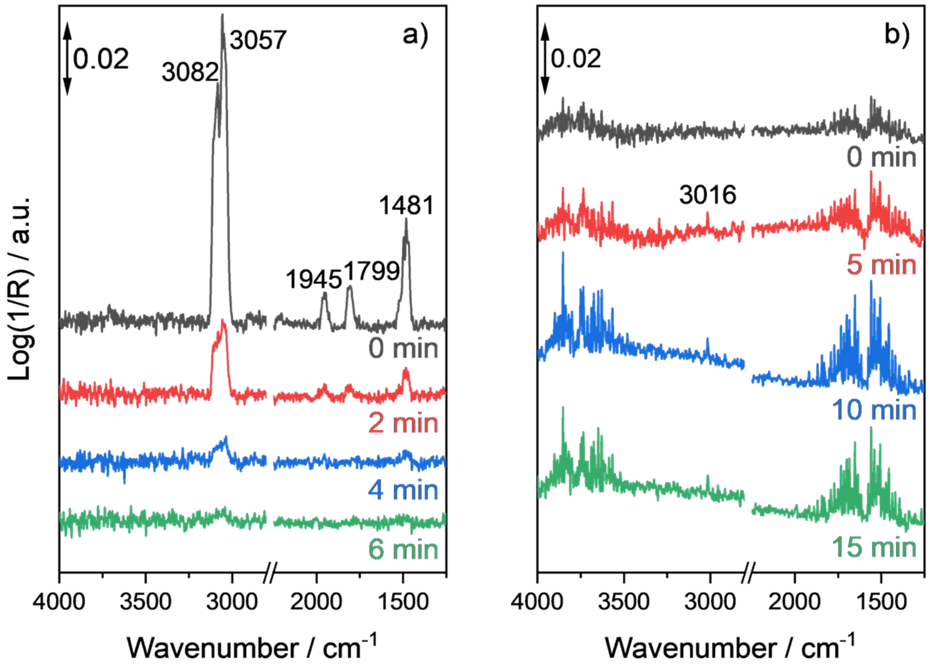

Figure SI 24: DRIFT spectra of a) benzene adsorption of Ni(5)MoO_3 in He and b) switch to H_2 at 325 °C.

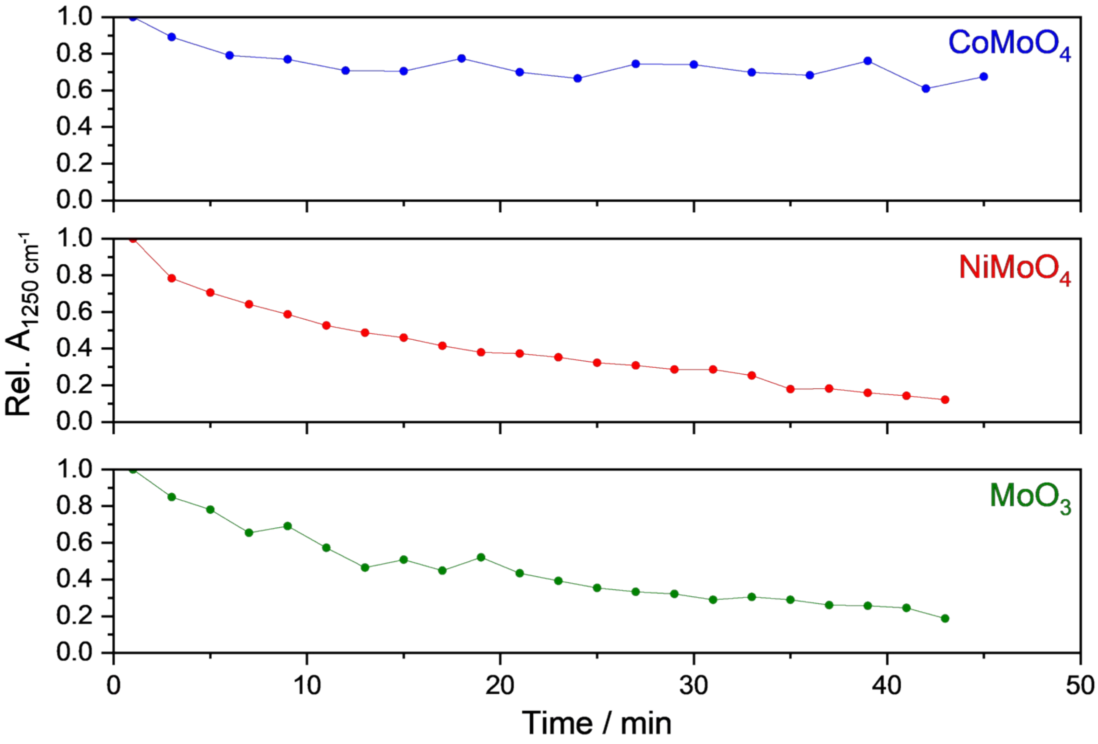

Figure SI 25: Relative integral values of absorption band at 1250 cm^{-1} at 325 °C in H_2.

SI-J: NH_3-adsorption transmission FTIR experiments

Surface acidity of the catalyst materials was analyzed by FTIR spectroscopy of adsorbed ammonia using a Tensor 27 spectrometer (Bruker) equipped with a heatable and evacuable IR reaction cell with CaF_2 windows, which was connected to a gas dosing and evacuation system. For each experiment, 50 mg of catalysts were pressed into self-supporting wafers with a diameter of 20 mm, which were first evacuated and then pretreated either in synthetic air or hydrogen (50 ml/min) at 325 °C for 120 min. After cooling to room temperature, a background spectrum was recorded and ammonia (5 vol.-% in helium) was introduced until saturation of adsorbed ammonia was achieved, followed by evacuation to remove physisorbed ammonia. The desorption of ammonia was followed by heating the sample in vacuum up to 300 °C and recording spectra every $\Delta\theta$ = 50 °C. For data analysis, subtracted spectra were used, obtained by the subtraction of a respective background spectrum from the ammonia adsorbate spectra.

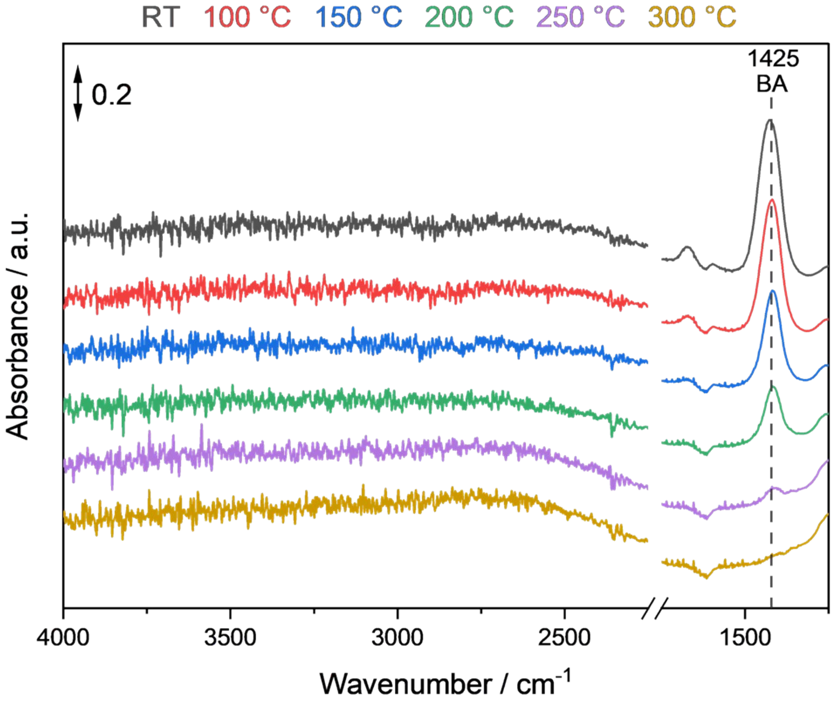

Figure SI 26: NH_3-adsoprtion transmission FTIR experiments of MoO_3 after reduction at 325 °C for 2 h in 100 % H_2.

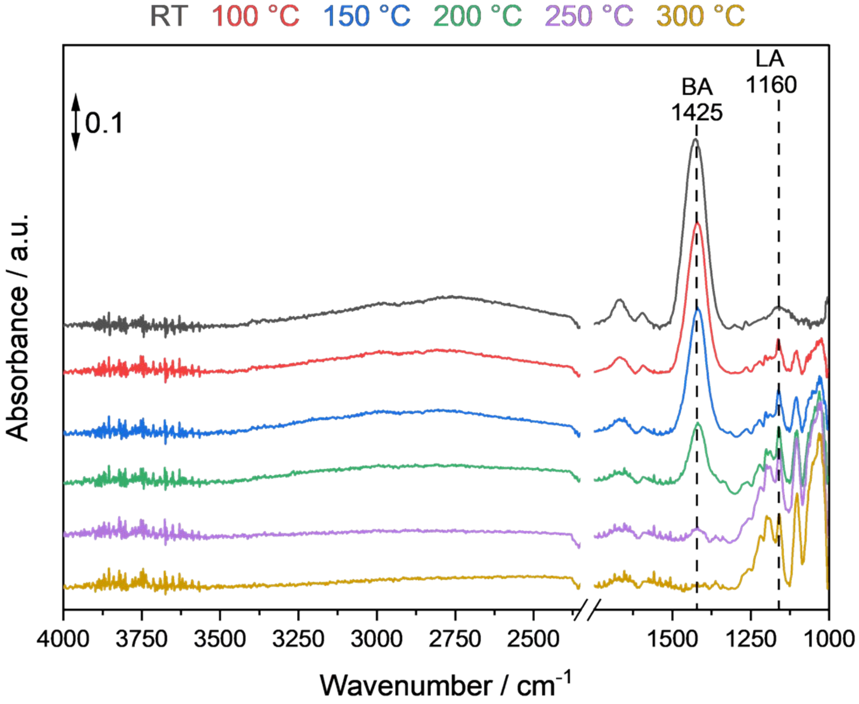

Figure SI 27: NH_3-adsoprtion transmission FTIR experiments of MoO_3 after calcination at 325 °C for 2 h in 100 % syn. air.

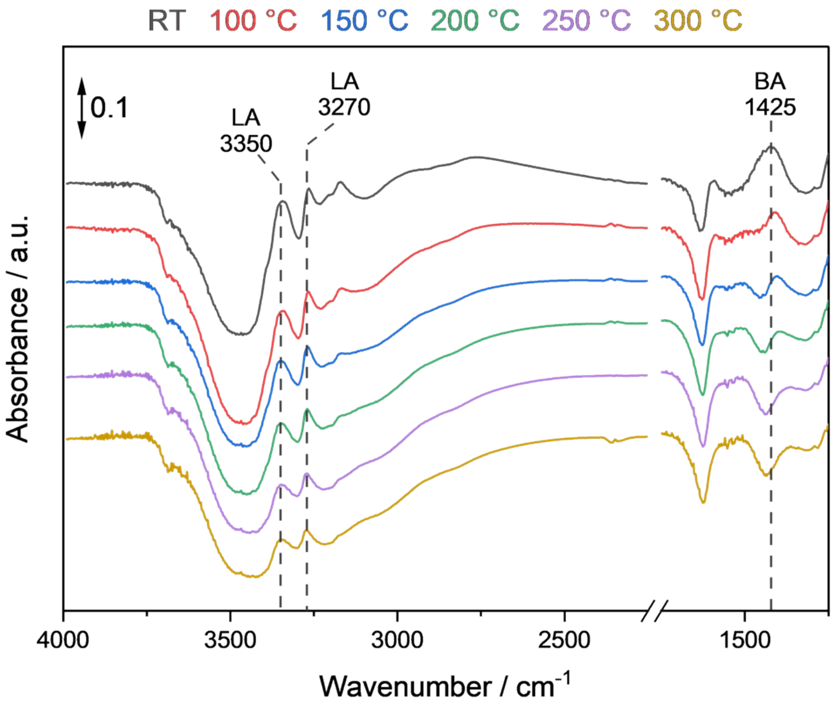

Figure SI 28: NH_3-adsoprtion transmission FTIR experiments of $NiMoO_4$ after reduction at 325 °C for 2 h in 100 % H_2.

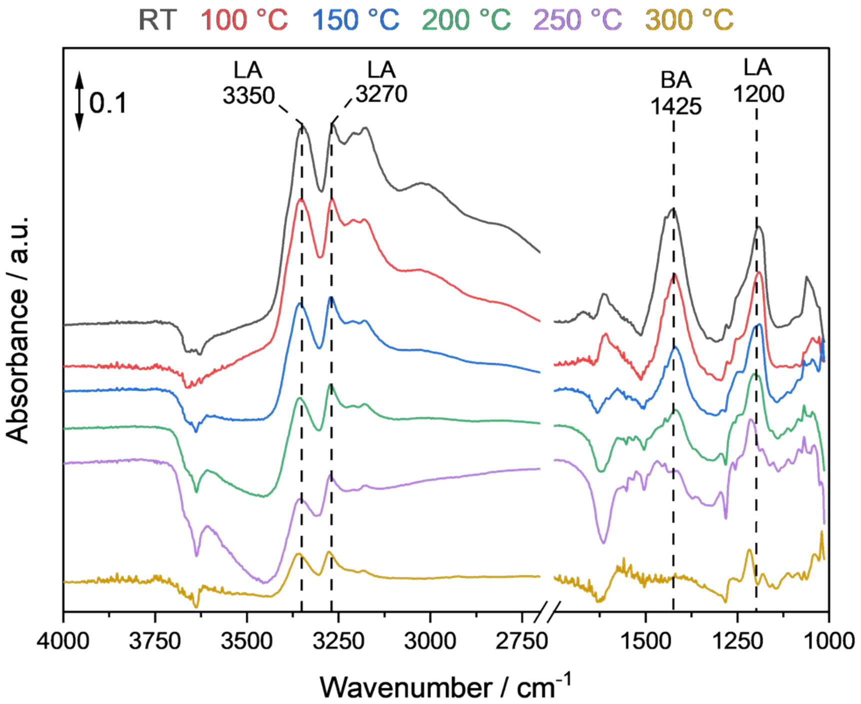

Figure SI 29: NH_3-adsoprtion transmission FTIR experiments of $NiMoO_4$ after calcination at 325 °C for 2 h in 100 % syn. air.

SI-K: In-situ XRD experiments

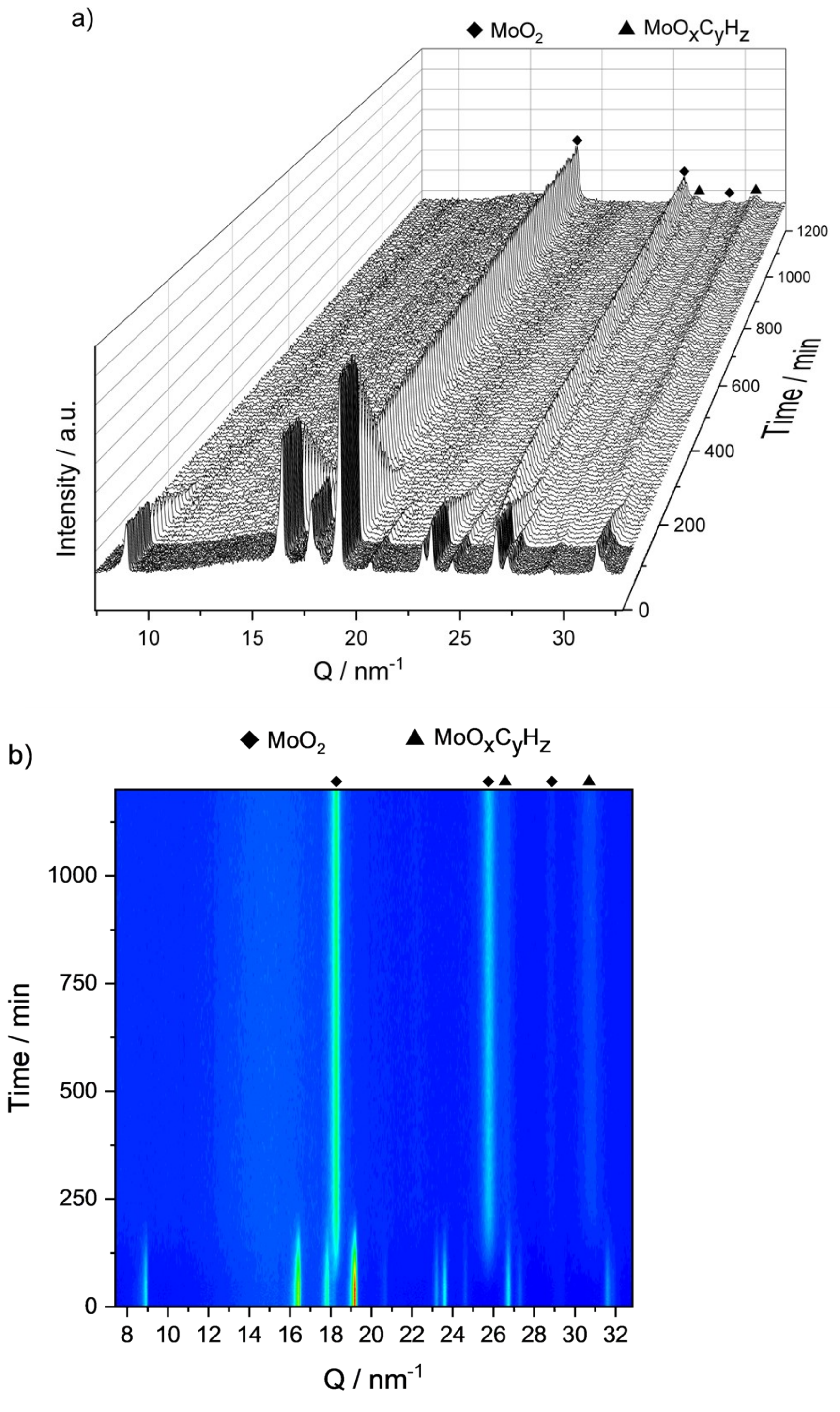

Figure SI 30: In-situ XRD of $MoO_xC_yH_z$ formation from MoO_3 in H_2:CH_4 (9:1) at 325 °C shown as a) waterfall plot and b) contour plot.

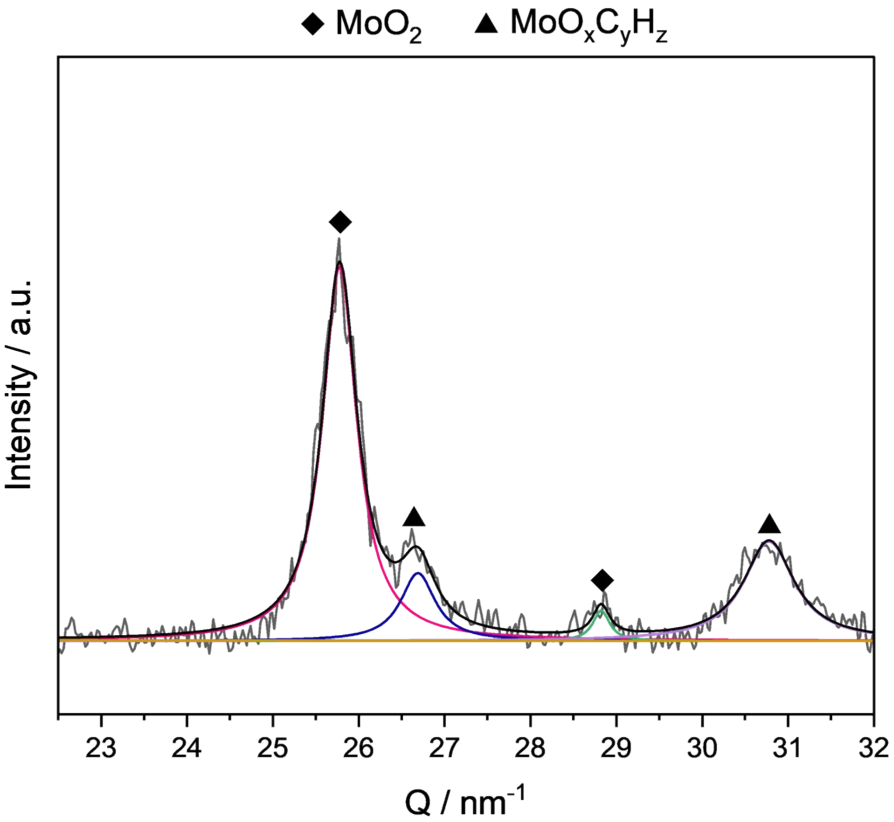

Figure SI 31: In-situ XRD of MoO$_x$C$_y$H$_z$ formation from MoO$_3$ in H$_2$:CH$_4$ (9:1) at 325 °C. Fitting results for MoO$_x$C$_y$H$_z$ and MoO$_2$ at 310 min.

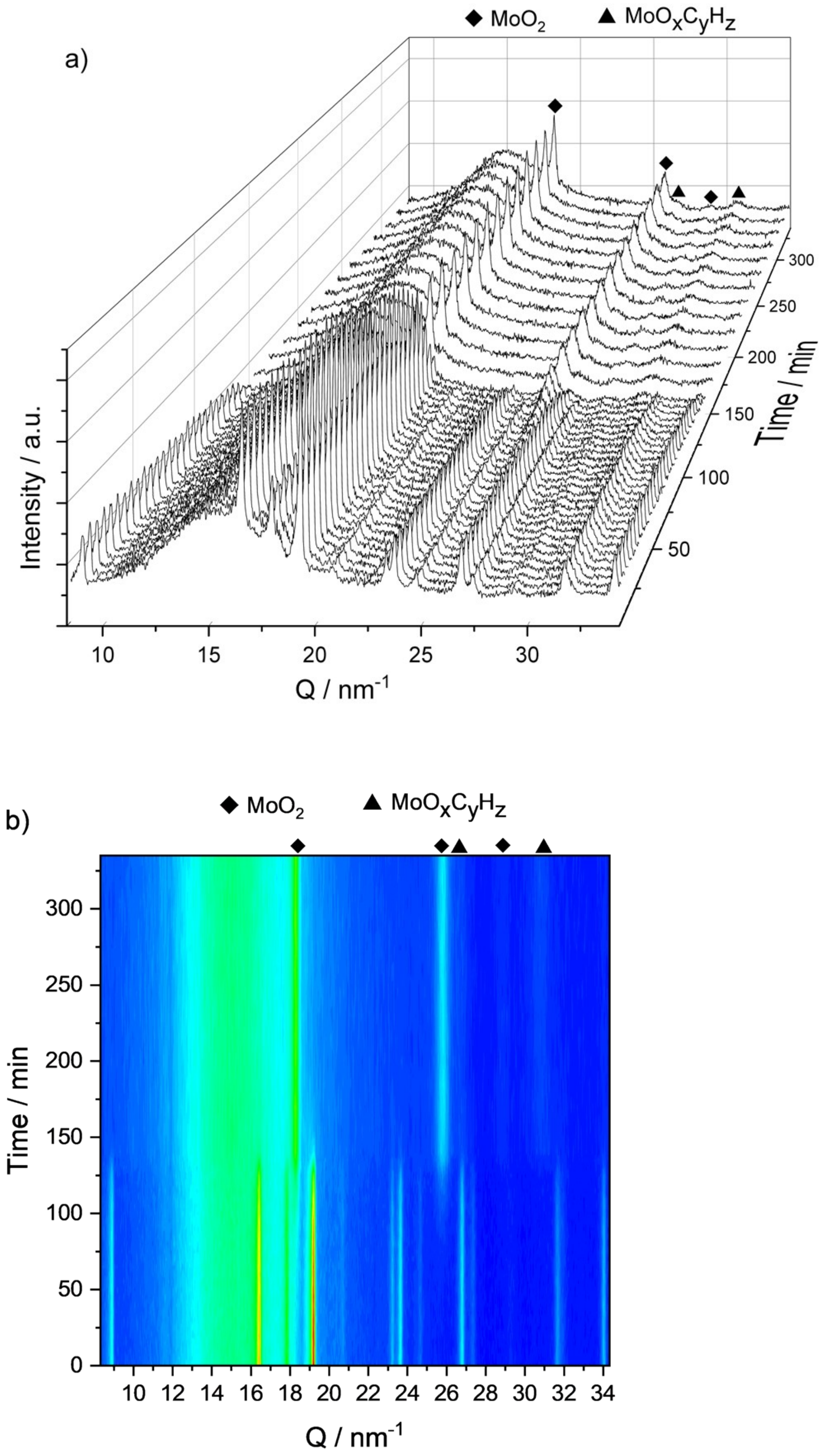

Figure SI 32: In-situ XRD of $MoO_xC_xH_z$ formation from MoO_3 in H_2:CH_4 (1:1) at 325 °C shown as a) waterfall plot and b) contour plot.

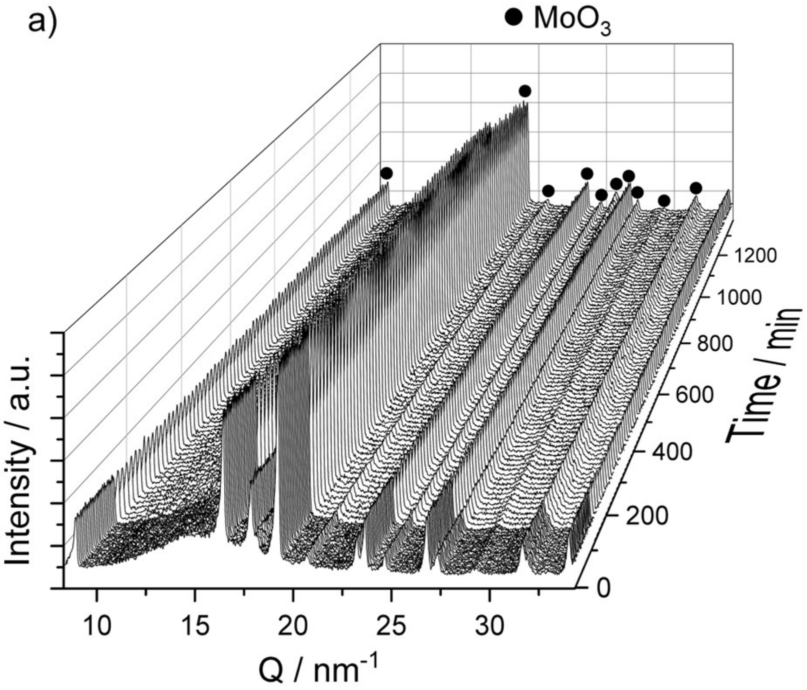

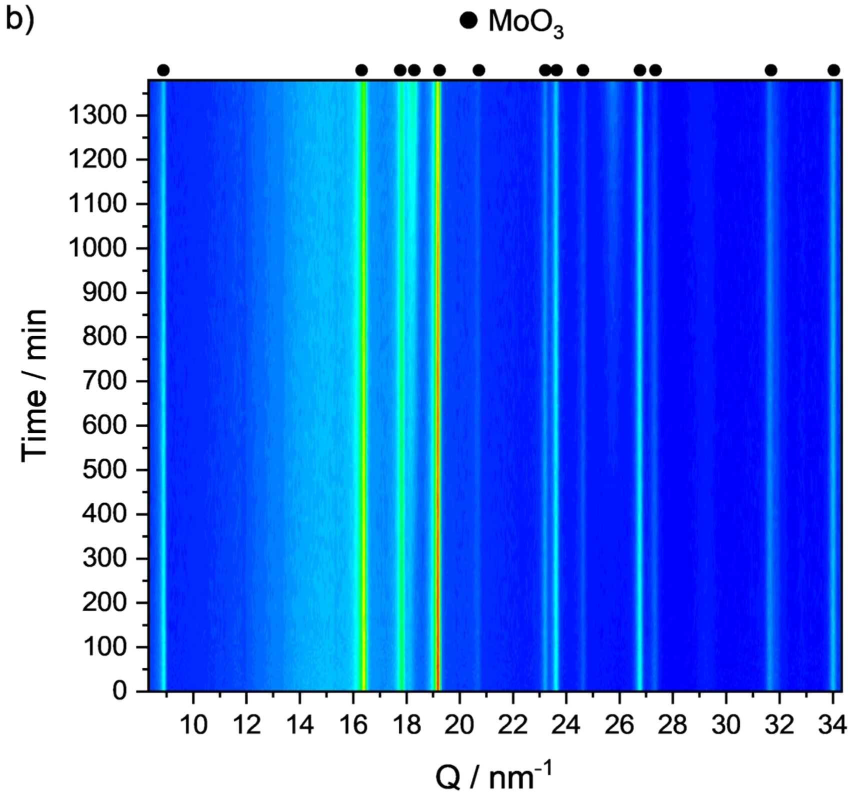

Figure SI 33: In-situ XRD of $MoO_xC_xH_z$ formation from MoO_3 in H_2:CH_4 (1:9) at 325 °C shown as a) waterfall plot and b) contour plot.

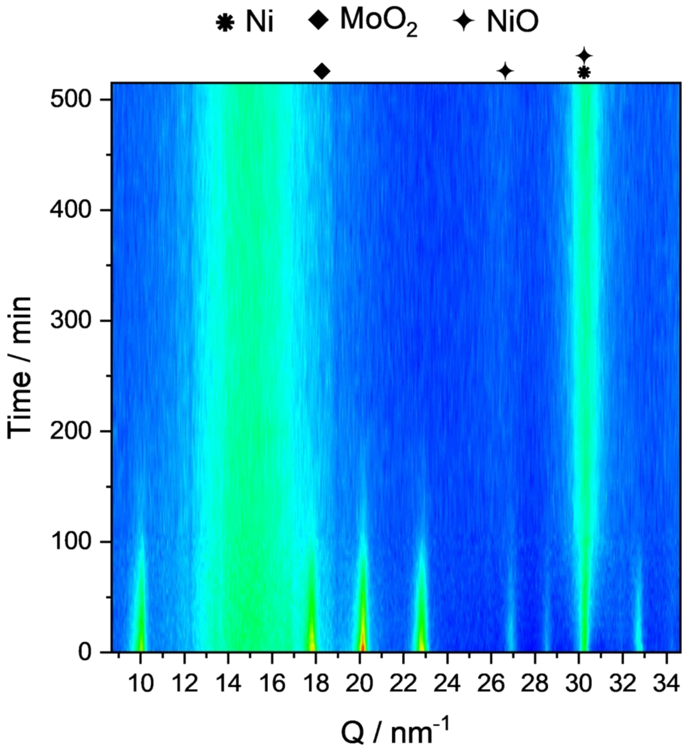

Figure SI 34: In-situ XRD reduction of $NiMoO_4$ in 100 % H_2 at 325 °C for 515 min.

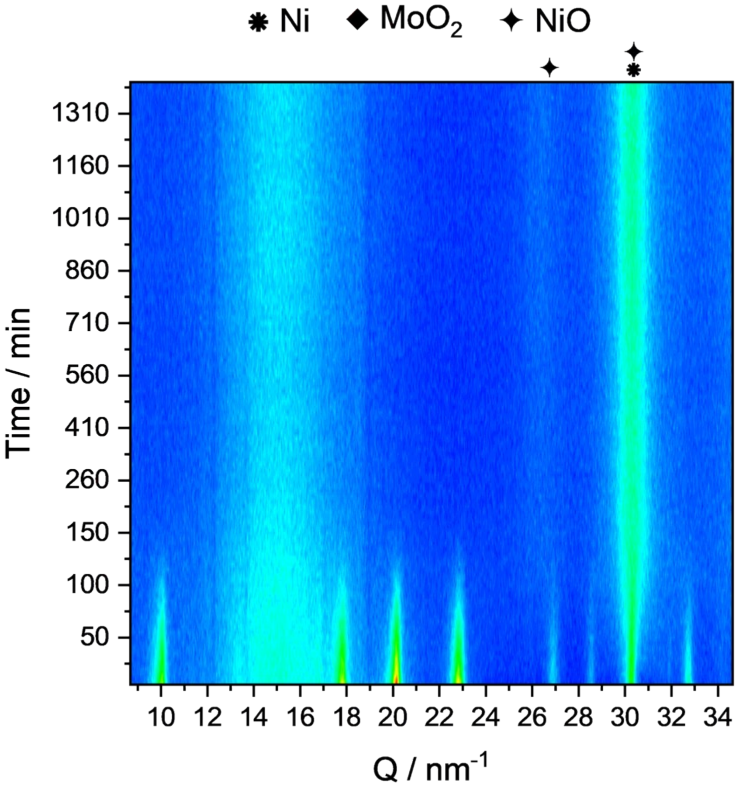

Figure SI 35: In-situ XRD of $NiMoO_4$ in H_2/CH_4 (9:1) at 325 °C for 1385 min.

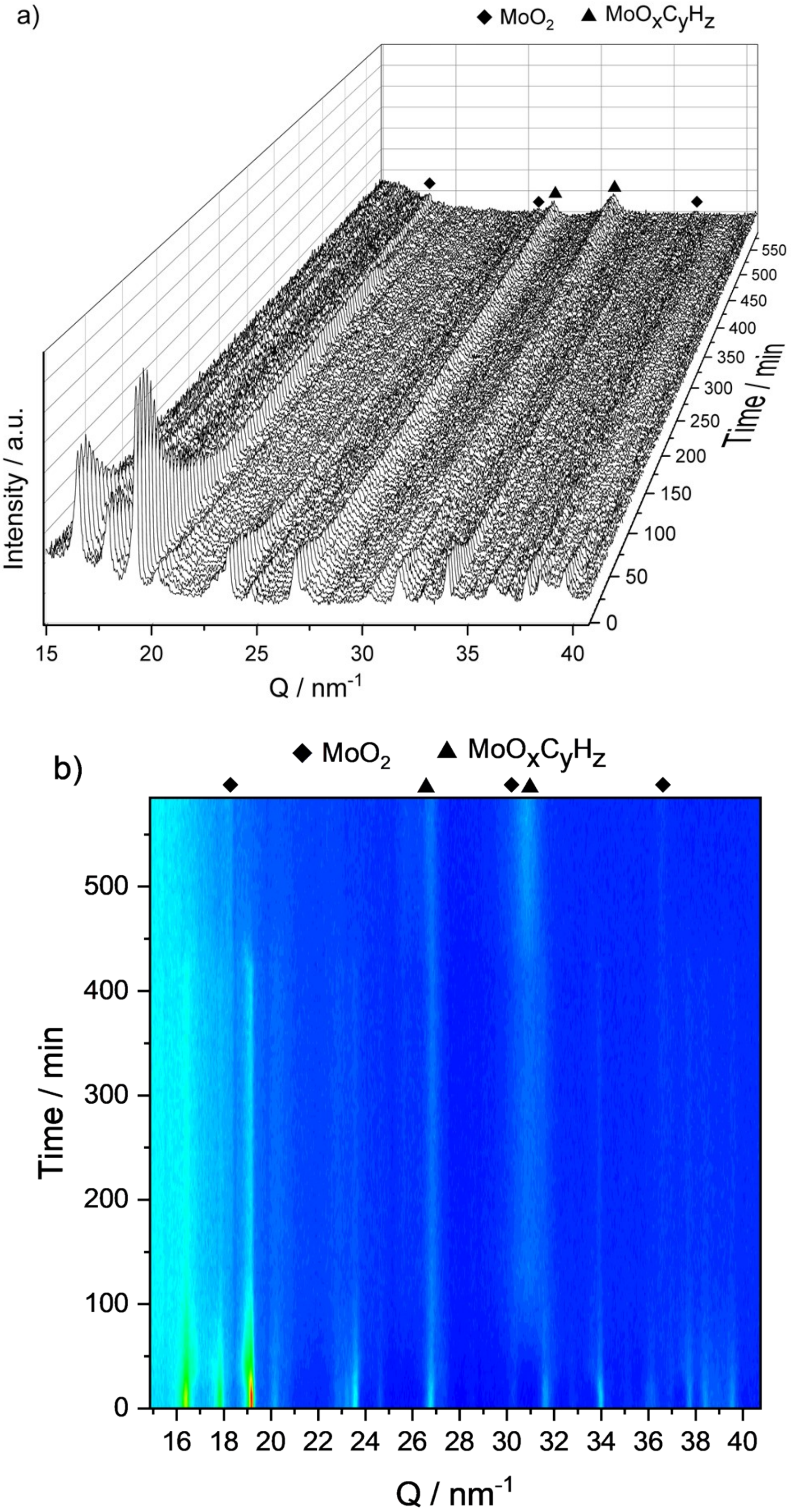

Figure SI 36: In-situ XRD measurement of Ni(5)MoO_3 heated up to 325 °C in He and switch to H_2 for 125 min followed by flushing with He and switch to CH_4 for 240 min. Afterwards, the sample was flushed again with He and treated for 160 min with H_2. Shown as a) waterfall plot and b) contour plot.

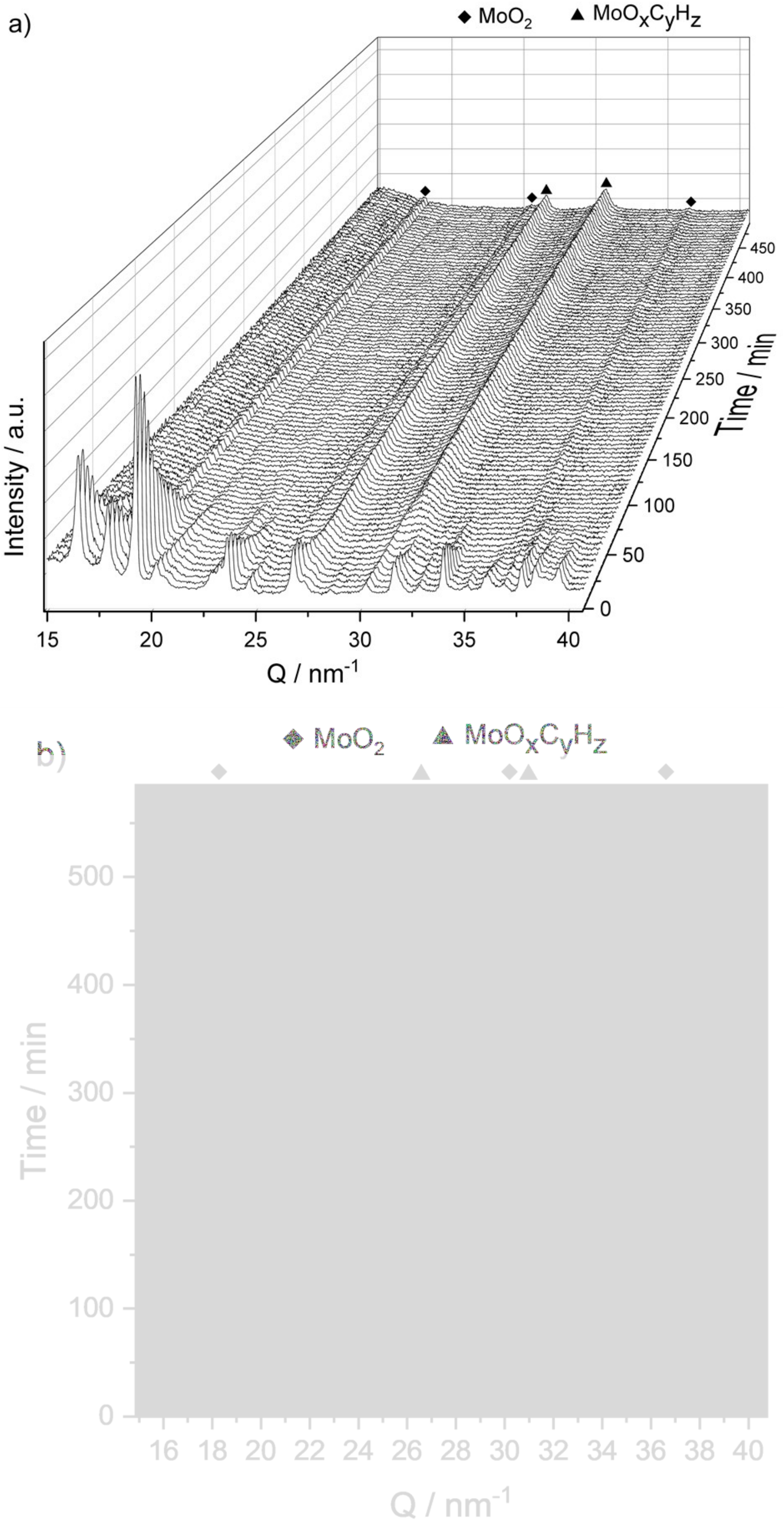

Figure SI 37: In-situ XRD measurement of Ni(5)MoO_3 in H_2/C_3H_6 (9:1) at 325 °C for 492 min shown as a) waterfall plot and b) contour plot.

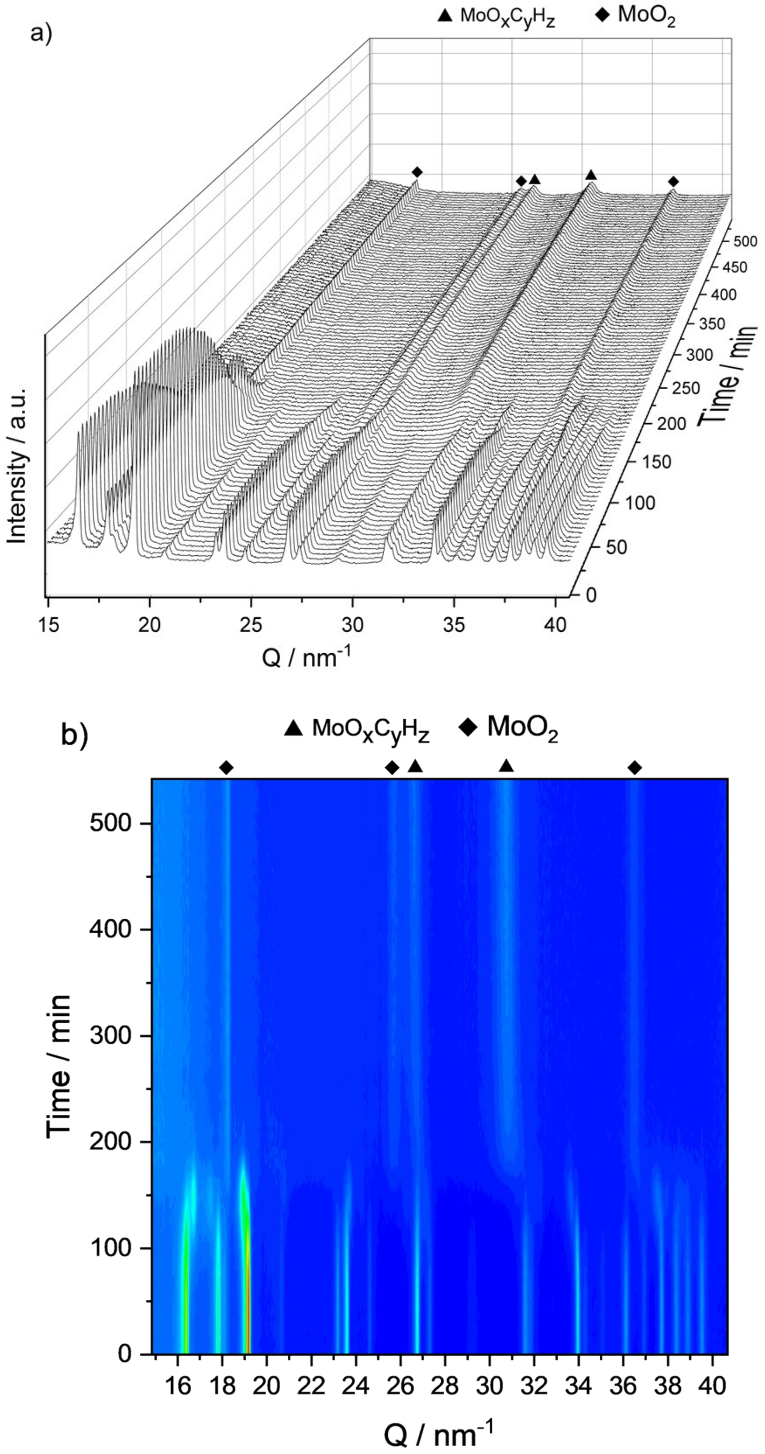

Figure SI 38: Two layered system with NiO and MoO_3 layer in H_2/C_3H_6 (9:1) at 325 °C for 542 min shown as a) waterfall plot and b) contour plot.

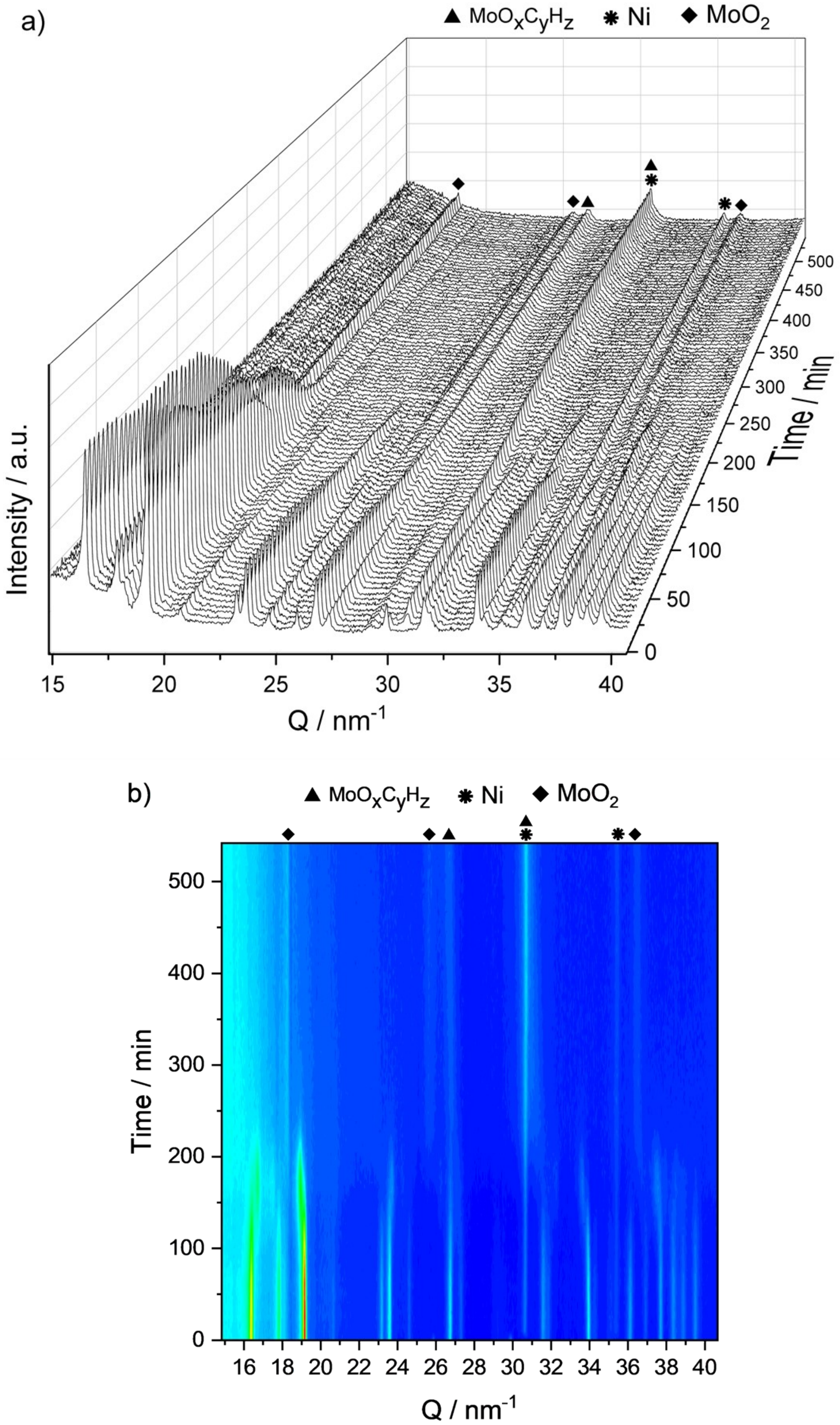

Figure SI 39: Physical mixture of NiO/MoO_3 in H_2:C_3H_6 (9:1) at 325 °C for 542 min shown as a) waterfall plot and b) contour plot.